International Active Matter Workshop 2026

VENUE:
Meiji University (Nakano Campus)

DATE:
23 - 24 January, 2026

Organiser

MEXT Joint Usage/Research Center Meiji University
"Center for Mathematical Modeling and Applications" (CMMA)

Co-organiser

JSPS Core-to-Core Program
"Advanced core-to-core network for the physics of self-organizing active matter"

Organising committee

Hiroyuki Ebata (Osaka Univ.)
Hiroyuki Kitahata (Chiba Univ.)
John Molina (Kyoto Univ.)
Nobuhiko J. Suematsu (Meiji Univ.)
Mitsusuke Tarama (Kyushu Univ.)
Ryoichi Yamamoto (Kyoto Univ.)

Web page

https://sites.google.com/view/activematter2026

Contact

email: active2026@googlegroups.com

Program

2026/1/23 Fri.

09:30 - 09:50	Registration
09:50 - 09:55	Opening remark
chair	Mitsusuke Tarama
09:55 - 10:55	**Carsten Beta** “Motility patterns and chemotaxis strategies of bacteria in porous media”
10:55 - 11:05	Break
chair	Hiroyuki Kitahata
11:05 - 11:25	**Yoshihito Uchida** “Designing topological edge states in bacterial active matter”
11:25 - 11:45	**Pyae Hein Htet Htet** “Hydrodynamic hovering of swimming bacteria”
11:45 - 13:00	Lunch
chair	Yuki Koyano
13:00 - 13:20	**Koshi Yoshida** “Distinct force pattern in dense assembly of deformable active cells”
13:20 - 13:40	**Hiroto Tomida** “Structural Changes in Active Crystals Induced by a Point Defect”
13:40 - 14:00	**Masaki Yoshida** “Elementary processes in active glasses”
14:00 - 14:20	**Masaki Itatani** “Enzymatic Reaction Network Generating Temporal pH Waveforms in Batch and Cell-sized Microcompartments”
14:20 - 14:40	**Norbert Német** “Monitoring of diffusion-controlled acid-base reaction in agarose gel matrix and its possible applications”
14:40 - 15:00	Group photo / Coffee break
15:00 - 16:40	**Poster presentations**
16:40 - 16:45	Break
chair	Masaki Itatani
16:45 - 17:45	**Istvan Lagzi** “Synthesis of crystalline materials from macro- to microscale”
18:00 - 20:00	Social meeting

2026/1/24 Sat.

09:30 - 09:50 Registration

chair John Molina

09:50 - 10:10 **Min-Jhe Lu**
"Dimensional Fate of Traveling Waves in Active Polar Media"

10:10 - 10:30 **Keisuke Taga**
"A Higher-Order Vicsek Model Emerging from Local Conformity"

10:30 - 10:50 **Chung Wing Chan**
"Emergent Collective Dynamics of Active Polar Particles in Heterogeneous Aligning Fields"

10:50 - 11:10 **Tsubasa Yoneda**
"Translational motion of droplet cluster under oscillatory shear"

11:10 - 11:30 Coffee break

chair Hiroyuki Ebata

11:30 - 11:50 **Airi Kato**
"Active particle in a thin interfacial droplet"

11:50 - 12:10 **Hiroyoshi Nakano**
"Collective Phenomena of Active Particles Communicating through Diffusion Fields"

12:10 - 12:30 **Hiroshi Noguchi**
"Spatiotemporal Patterns in Active Potts Models"

12:30 - 13:30 Lunch

chair Kento Yasuda

13:30 - 13:50 **Tamao Maeda**
"The Spatial Structure of Horse Social Groups"

13:50 - 14:10 **Riccardo Muolo**
"Swarming in 1-dimension: an empirical and numerical study on Iriomote-native soldier crabs"

14:10 - 14:30 **Sota Inoue**
"Filamentous and dynamic raft structures in seabirds"

14:30 - 14:50 Coffee break

chair Airi Kato

14:50 - 15:50 **Katsuhiro Nishinari**
"Crowd management and active matter control in reality"

15:50 - 16:00 Closing remark

==========

Presentation time

Invited lectures: 60 min each, <u>including discussions</u>

Contributed talks: 20 min presentation, <u>including discussions</u>

Poster list

1. **Yuma Hida**, “Physical reservoir computing using the Vicsek model”
2. **Takuma Hisamatsu**, “Crystal stability of active matter”
3. **Akito Saito**, “How do topological defects of cell sheet reorient under external fluid flow?”
4. **Kei Oriyose**, “Rectification of Active Brownian Particles in a 1D periodic ratchet”
5. **Liliana KERSHNER**, “Just keep swimming: electrokinetic Janus particles under external fluid flow”
6. **DUC DAM**, “Jamming Transition of Chiral Active Particles”
7. **Subhodeep Dey**, “Phase Diagram of Chiral Active Brownian Particles”
8. **Yuki Hirota**, “Defect structure and dynamics in active nematic membranes”
9. **Daisuke Miyokawa**, “Numerical simulation of active nematics in complex geometries with the Beris-Edwards model”
10. **Daisuke Katayama**, “Mechanical model of cell crawling with torque-free rotation”
11. **Ryunosuke Karimata**, “Self-aligned tension gradient induces antiparallel circulation pattern in confluent cell monolayers”
12. **Naoyasu Morino**, “Euglena’s Phototaxis and Bioconvection under Multiple Light Sources”
13. **Ryuhei Itoh**, “Motility analysis of the density wave propagation in Ciliate Tetrahymena suspension”
14. **Sohei Nakamura**, “Cellular-Scale Mechanism of Optimal Substrate Stiffness for Cell Crawling”
15. **Nen Saito**, “Collective Dynamics of Highly Packed Elliptical Cells”
16. **Akinari Tomiie**, “Synchronous beating of cardiac cells by elastic interactions”
17. **Keigo Takeda**, “Phototaxis of the Self-propelled Droplet -- Stochastic Response to the Light Intensity Gradient”
18. **Shinya Hakuta**, “Light-written reconfigurable active matter with memory: optically creating, coupling, and erasing self-propelled droplets”
19. **Yuki Koyano**, “Coalescing dynamics of self-propelled droplets on substrates”
20. **Lintao LIU**, “Topological Defects in Spiral Wave Chimera States”
21. **Yuta Tateyama**, “Global bifurcation analysis of nonreciprocal pattern transitions near O(2)-symmetric Takens-Bogdanov point”
22. **Mizuki Nakamura**, “Pattern selection mechanism depending on initial conditions in immiscible two-layer thermal convection”
23. **Kento Yasuda**, “Onsager–Machlup variational principle for active systems”

24. **John Molina**, “Dual Hamiltonian/Lagrangian Learning”
25. **Hugh Shearer Lawson**, “Chemical Resonance, Beats, and Frequency Locking in Forced Chemical Oscillatory Systems”
26. **Tianjing Zhou**, “Traveling defects as a precursor of the chimera states in a chain of non-locally coupled oscillators”
27. **Yusei Kitagaki**, “Direct numerical simulations of Quincke Rollers in a bulk 3D system”
28. **Shota HOSONO**, “The Effects of Ordinary Viscosity in Chiral Shallow Water Model”
29. **Bokusui Nakayama**, “Autonomous Noise-Rectified Locomotion via Self-Generated Viscosity Asymmetry”
30. **Simon Kaspar Schnyder**, “Altruism in Epidemics”
31. **Sakurako Tanida**, “Exploring How We Explore: Statistical Patterns of Indoor Walking in Interactive Spaces”
32. **Nobuhiko Suematsu**, “Stochastic Response of a Self-propelled Particle in the Chemical Concentration Gradients”

Core poster presentation time:

Odd numbers → 15:00 - 15:50
Even numbers → 15:50 - 16:40

Abstracts

Day 1
23 Jan., 2026 (Fri.)

Motility patterns and chemotaxis strategies of bacteria in porous media

S. Beier[1], A. Datta[1], V. Pfeifer[1], R. Großmann[1] and C. Beta[1,2]

[1]Institute of Physics and Astronomy, University of Potsdam, Germany
[2]Nano Life Science Institute (WPI-NanoLSI), Kanazawa University, Japan

Elucidating the basic mechanisms underlying bacterial motility and navigation is essential for understanding processes such as the spreading of infectious diseases or the development of biofilms. A central challenge for motile bacteria is to navigate their natural habitats, which are often composed of complex and structured environments such as tissue or soil. In this presentation, we investigate the connection between microscale locomotion strategies of bacteria and their macroscopic transport behavior in heterogeneous media, considering both unbiased motion in porous environments and directed migration in response to chemical gradients. Our approach combines laboratory experiments with active particle modeling, relying on the soil-dwelling bacterium *Pseudomonas putida* as a model organism.

We first investigate how the presence of a disordered medium, such as agar, modifies the run-and-turn pattern known from bacterial swimming in homogeneous liquid environments. We uncover striking changes in motility, including transient subdiffusive dynamics that arise from intermittent mechanical trapping events characterized by power law-distributed trapping times. In addition, we demonstrate that *Pseudomonas putida* is capable of chemotactic migration within porous media, despite a strongly reduced mean free path length. Unlike chemotaxis in uniform fluids — where directional movement is largely achieved by adjusting run durations depending on the swimming direction — we identify an alternative chemotactic mechanism in porous settings. Specifically, bacteria bias their reorientation angle during turning events, thereby preferentially aligning subsequent runs toward the source of chemoattractant. Active particle simulations, informed by experimentally measured swimming statistics, reveal that this turn-angle bias constitutes the dominant chemotactic strategy in porous environments.

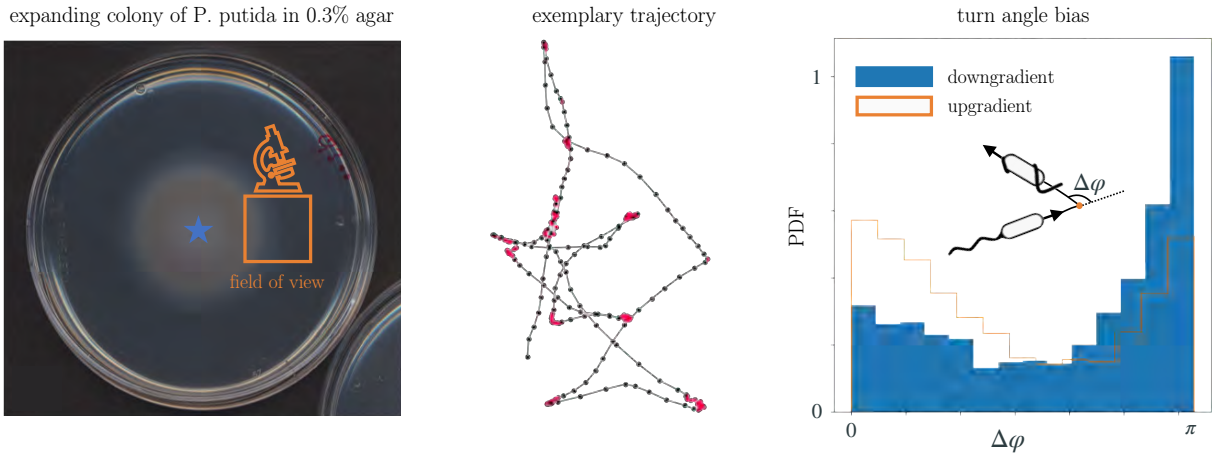

Figure 1: Left panel: expansion of a bacterial colony in agar; middle panel: exemplary trajectory of a bacterium, recorded at the edge of the expanding colony as indicated on the left; right panel: turn angle bias, i.e., bacteria can tune their turning angle depending on the orientation of the preceding run with respect to the chemical gradient.

References

1. A. Datta, S. Beier, V. Pfeifer, R. Großmann, and C. Beta, *Sci. Rep.* 15, 20320 (2025).
2. A. Datta, C. Beta, and R. Großmann, *Phys. Rev. Res.* 6, 043281 (2024).
3. S. Beier, V. Pfeifer, A. Datta, R. Großmann, and C. Beta, arXiv:2503.05286.

Designing topological edge states in bacterial active matter

Yoshihito Uchida[1], **Daiki Nishiguchi**[2], **Kazumasa A. Takeuchi**[1,3,4]

[1]Department of Physics, The University of Tokyo
[2]Department of Physics, Institute of Science Tokyo
[3]Universal Biology Institute, The University of Tokyo
[4]Institute for Physics of Intelligence, The University of Tokyo

While active matter is intrinsically nonequilibrium and fluctuating, the emergence of topologically protected edge states with characteristic transport has been theoretically proposed using the methodology of wavenumber topology. However, experimental realization remains largely unexplored, having been limited to systems composed of chiral active particles. Extending such edge states to geometrically structured systems offers new routes to realize and control topological transport in active matter. Here, using microfabricated kagome-type geometrical structures, we realized topological edge states in dense bacterial suspension. The structures consist of circular wells connected by ratchet-shaped channels that induce unidirectional flow (Fig. 1). Then we found edge localization of bacterial density, resulting from collective flow driven by the network geometry. Using theoretical modeling, we also unveiled the topological origin of the observed edge states. By tuning the geometry of the microfabricated devices, we identified key geometrical features for the emergence of edge states. Our experimental findings will pave the way toward establishing a foundation for controlled topological transport in such active matter.

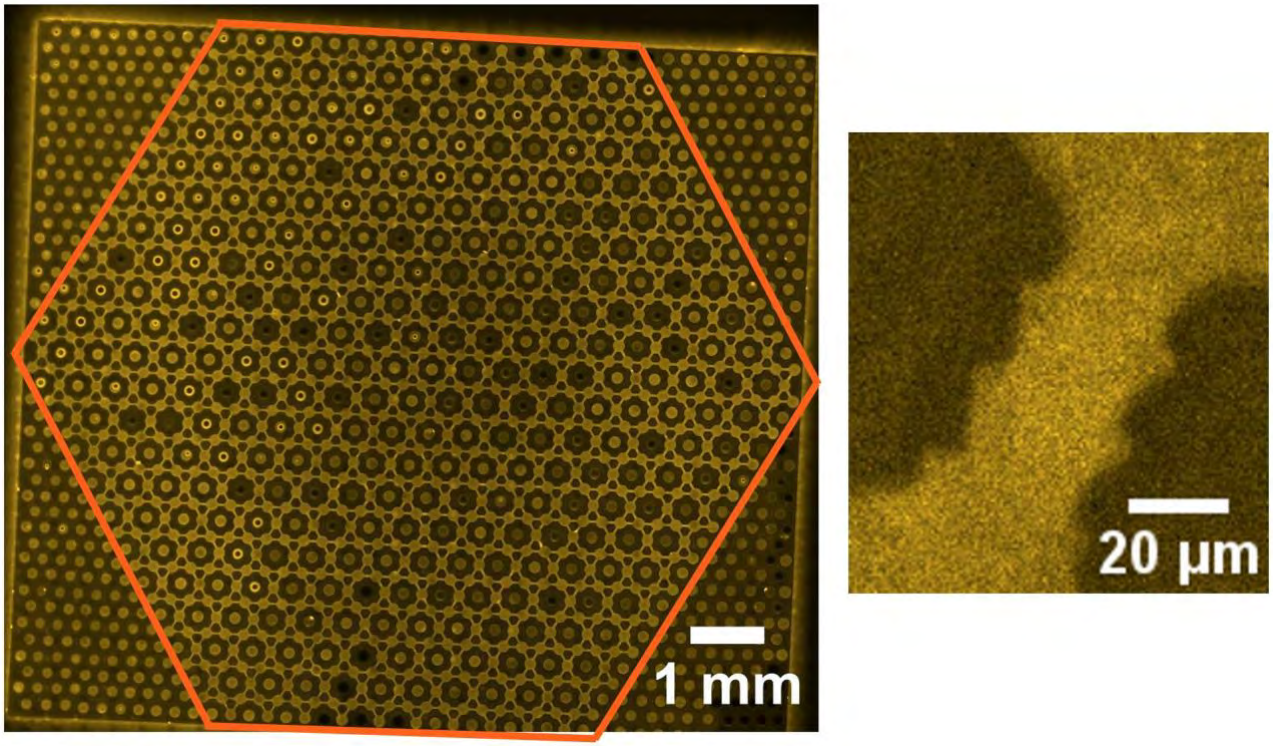

Fig. 1: Epifluorescence microscopy image of dyed bacterial suspension confined in a directional kagome network (left), which is composed of wells connected by ratchet-shaped channels (right).

Acknowledgements
We thank T. Yoshida, T. Sagawa, Y. Ashida, and K. Sone for valuable discussions. This work is supported in part by JSPS KAKENHI (JP19H05800, JP20K14426, JP23K25838, JP24K00593, JP25K22005), JST FOREST (JPMJFR2364), JST PRESTO (JPMJPR21O8), JST SPRING (JPMJSP2108), JSPS Core-to-Core Program (JPJSCCA20230002), and FoPM (Univ. Tokyo).

Hydrodynamic hovering of swimming bacteria

Pyae Hein Htet[1], **Debasish Das**[2], **Eric Lauga**[3]

[1]Department of Mathematics, Kyoto University
[2]Department of Mathematics and Statistics, University of Strathclyde, Glasgow
[3]Department of Applied Mathematics and Theoretical Physics, University of Cambridge

Flagellated bacteria are hydrodynamically attracted to rigid walls, yet past work shows a "hovering" state where they swim stably at a finite height above surfaces. We use numerics and theory to reveal the physical origin of hovering. Simulations first show that hovering requires an elongated cell body and results from a tilt away from the wall. Theoretical models then identify two essential asymmetries: the response of width-asymmetric cells to active flows created by length-asymmetric cells. A minimal model reconciles near- and far-field hydrodynamics, capturing all key features of hovering.

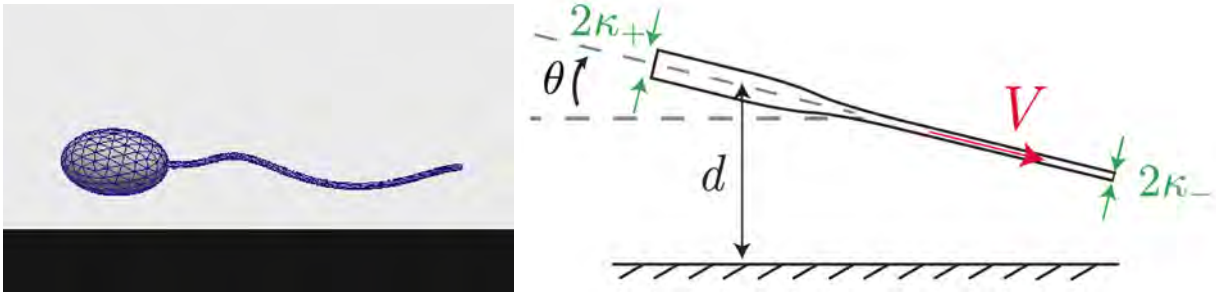

Fig 1: Left: Snapshot from boundary element method simulations showing a flagellated bacterium stably hovering above a rigid wall. Right: a theoretical model shows that this phenomenon emerges from simple geometrical asymmetries.

References

Htet, P. H., Das, D., & Lauga, E: "Hydrodynamic hovering of swimming bacteria above surfaces", *Physical Review Research*, **6**(3), L032070 (2024).

Distinct force pattern in dense assembly of deformable active cells

Koshi Yoshida[1], **Nen Saito**[2], **Shuji Ishihara**[1], **Kaoru Sugimura**[1]

[1]The University of Tokyo
[2]University of Tsukuba

Diverse phenomena manifest themselves in active matter, especially in its dense assembly. Recently, several models have been developed to express deformation in cells, and intriguing properties have been found at high density including intermittent behaviors[1]. However, mechanical features like force network, well investigated in passive systems, are yet to be understood. Therefore, the target of this study is to unveil the effect of deformability in self-propelled cells on the mechanical interaction with each other. To this end we simulated deformable cells which are modeled as a single-valued function representing the radial distance to the contour, expanded via a Fourier series[2]. At a fixed density of $\rho = 1$, we focused on the propulsion force v_0 and the tension parameter η as control parameters.

One of the key findings is the distribution of force strength between cells displaying multiple peaks (Fig1A, B) at weak tension, which was previously not observed even in passive systems. This result clearly differs from the assembly with strong tension, which exhibited a Gaussian-like unimodal force distribution. The network of force transmission was analyzed by Topological Data Analysis. The persistence diagrams (PDs) constructed upon the force network via inverse Vietoris-Rips filtration showed stark differences as the phase transitions from solid to liquid (Fig1D1-5). Notably, the formation of a cluster far from the diagonal line indicates strong force loops each enclosing weak force centers. Such weak interactions, distinguished by a Gaussian Mixture Model, are dominant especially with weak tension η and modest propulsion force v_0 slightly above the boundary line of the phase as seen in Fig1C.

The curvature constraint, associated with the finite Fourier modes, was found to play a role in the formation of weakly interacting pairs of cells. The system size (in)dependency of this phenomenon is discussed in relation to the intermittent dynamics, as well as biological implications.

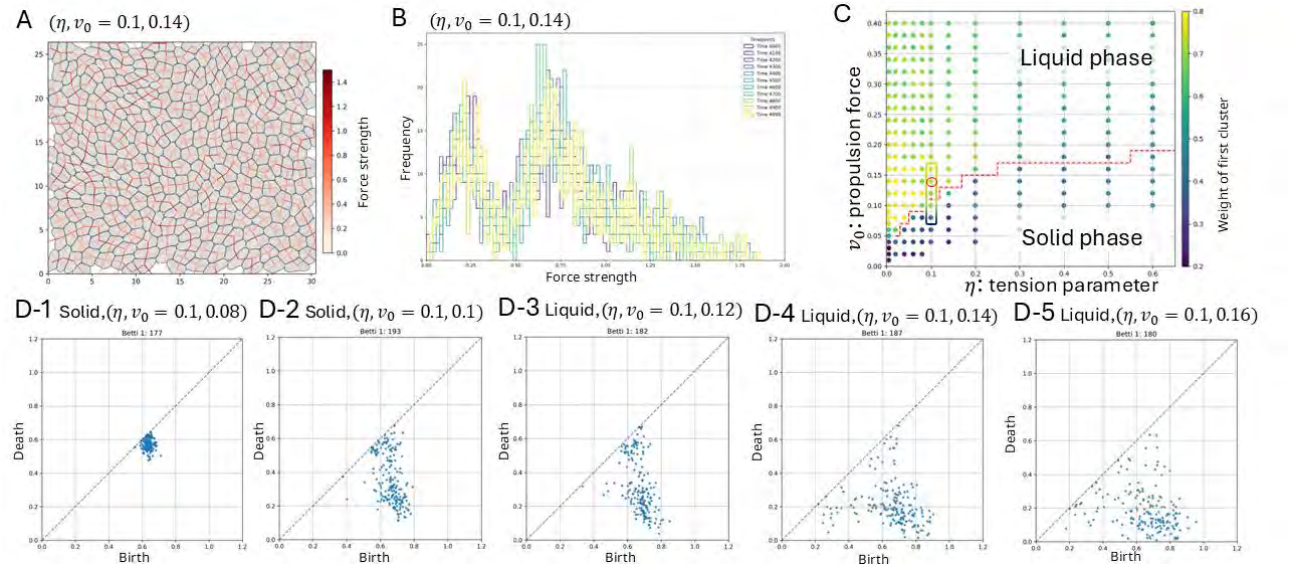

Fig 1. A: Typical snapshot, B: force distribution, C: Phase diagram, D: PDs of force network

References

1. Loewe, B., Chiang, M., Marenduzzo, D., & Marchetti, M. C., *Physical Review Letters*, **125**, 3(2020)
2. Saito, N., and Ishihara, S., *Science Advances* **10**, 19 (2024).

Synchronous beating of cardiac cells by elastic interactions

Akinari Tomiie, Nariya Uchida
Department of Physics, Graduate School of Science, Tohoku University

The pumping function of the heart is maintained by the synchronous beating of numerous cardiomyocytes. Recent experiments suggest that sarcomeres, the contractile units of cardiomyocytes, synchronize not only through biochemical signals but also via elastic mechanical interactions [1]. Previous studies have examined the stability of in-phase and anti-phase synchronization with respect to cell orientation using static elastic energy analyses that model cardiomyocytes as force dipoles [2].

In the present study, we extend this approach and develop a mathematical model to describe the dynamics of mechanically driven synchronization. The actomyosin contractile mechanism of the sarcomere is well described by the following nonlinear equation:

$$\ddot{x_i} - \varepsilon\left(1 - \dot{x_i}^2\right)\dot{x_i} + x_i = f_{\mathrm{int}} \tag{1}$$

Here, x_i denotes the displacement of the cardiac cell i from its natural length. The second term represents energy injection via ATP hydrolysis at low velocities and dissipation at high velocities. The force f_{int} arises from the interaction with other cells. Equation (1) with $f_{\mathrm{int}} = 0$ is known as the Rayleigh equation and exhibits a limit cycle.

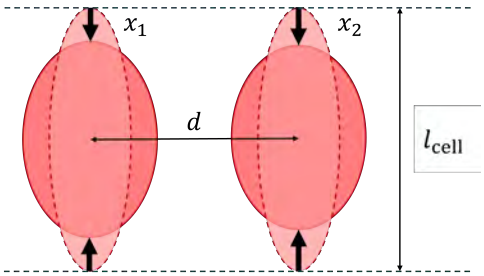

Fig.1: Schematic picture of two cardiomyocytes arranged side-by-side, with the natural cell length l_{cell}, intercellular distance d, and displacements x_1, x_2.

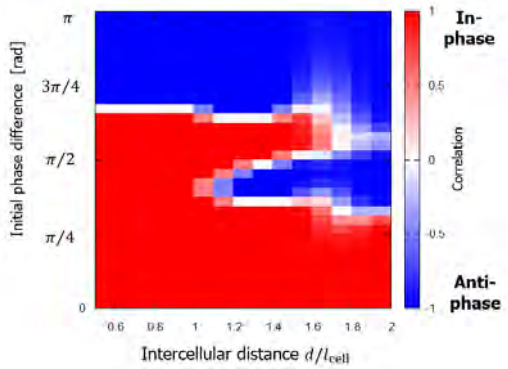

Fig.2: Dependence of the final synchronized states (red: in-phase, blue: anti-phase) on the initial phase difference and intercellular distance.

We consider a system of two cardiomyocytes placed on a semi-infinite elastic substrate with various relative orientations. Contraction of the cells induces deformation of the elastic medium, resulting in mechanical interaction. For the configuration shown in Fig.1, we find numerically that either the in-phase or anti-phase synchronization is achieved depending on the initial phase difference and the intercellular distance, as shown in the state diagram (Fig.2). The bistability suggests the importance of dynamical modeling of synchronous beating beyond energy minimization principle.

References

[1] I. Nitsan *et al.*, *Nat. Phys.* **12**, 472–478 (2016).
[2] O. Cohen and S. A. Safran, *Soft Matter* **12**, 6088–6095 (2016).

Elementary processes in active glasses

Masaki Yoshida, Hideyuki Mizuno, Atsushi Ikeda

The University of Tokyo

To understand the glassy dynamics of dense active matter, it is necessary to develop a microscopic understanding of the rearrangements of particles in dense active matter. In thermal systems, we can discuss this problem based on the firm ground: the rearrangements are described as the activation process in the energy landscape [1]. The transition path is determined by the steepest descent from the saddle point, and the transition rate follows the Kramers' law [2]. However, for active systems, neither the transition path nor the transition rate have been fully clarified.

In this study, we use molecular dynamics simulations and theoretical analysis to investigate the transition paths and transition rates of the particles' rearrangements in glassy states of active Ornstein-Uhlenbeck particles. We consider binary Lennard-Jones particles driven by external Ornstein-Uhlenbeck noises. We first performed the energy landscape analysis of the model. We calculated the inherent structures, saddle points, and the energy barriers by using the FIRE algorithm and the nudged elastic band method. Then, we performed molecular dynamics simulations to measure the mean-first passage time for the transition from an inherent structure to another. By analyzing these data, we identified the law that the mean first-passage time in active systems follows. While the transition rate is dominated by the energy barrier in thermal systems, it is dominated by the square of the force magnitude in active systems. Our results suggest that the dynamics of active glasses can be described based on the W-landscape rather than the potential energy landscape, where W is defined as the square of the force magnitude.

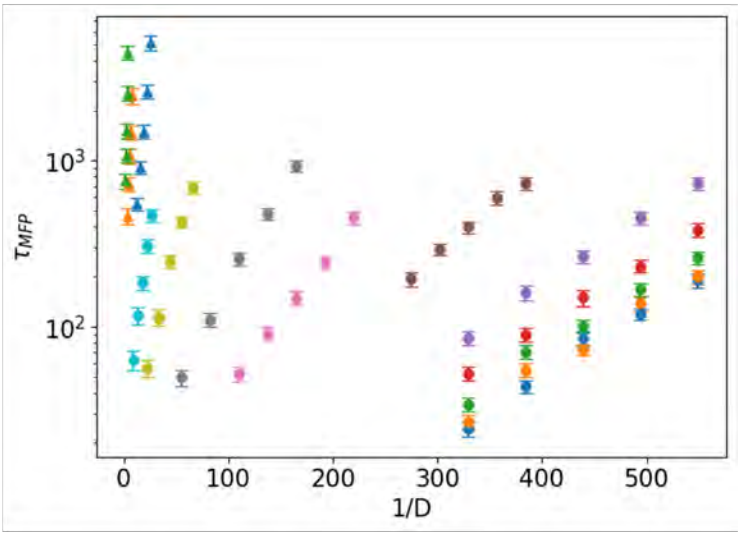

Fig.1：Timescale of particle rearrangements from a given configuration as a function of the energy scale of the active noise D. Different colored symbols correspond to different persistence times τ.

Acknowledgements
We acknowledge Prof. Peter Sollich for the discussion.

References

1. M. Goldstein: "Viscous Liquids and the Glass Transition: A Potential Energy Barrier Picture", Journal of Chemical Physics, 51, 3728–3739 (1969).
2. H. A. Kramers: "Brownian motion in a field of force and the diffusion model of chemical reactions", Physica 7, 284–304 (1940).

Enzymatic Reaction Network Generating Temporal pH Waveforms in Batch and Cell-sized Microcompartments

Masaki Itatani[1], Paola Albanese[2], Nadia Valletti[2], Gábor Holló[3], Sándor Kurunczi[4], Robert Horvath[4], Federico Rossi[2], and István Lagzi[5,6]

[1]Department of chemistry, Faculty pf Science, Hokkaido University, Japan
[2]Department of Earth, Environmental and Physical Sciences, University of Siena, Italy
[3]Department of Fundamental Microbiology, University of Lausanne, Lausanne, Switzerland
[4]Institute of Technical Physics and Materials Science, HUN-REN Centre for Energy Research
[5]Department of Physics, Institute of Physics, Budapest University of Technology and Economics, Hungary
[6]ELKH-BME Condensed Matter Research Group, Budapest University of Technology and Economics , Hungary

The design of reaction networks that exhibit autonomous and recursive pH changes, which is ubiquitous in living systems, is a crucial strategy for developing smart materials, as such systems can be readily integrated with a wide range of bio-related molecular self-assembly processes. However, autonomous chemical reaction systems of this type have so far been largely limited to a few classical chemical oscillators, such as the Belousov–Zhabotinsky reaction, typically operated under open-system conditions. In this study, we constructed an enzymatic reaction network that exhibits autonomously recursive pH changes within a mild pH range by coupling two antagonistic enzymatic reactions that generate H^+ and OH^-, namely the urea–urease and ester–esterase reactions. The fundamental properties of the designed system were investigated in a batch reactor, where it displayed temporal pH waveforms over a range spanning neutral to weakly basic conditions (Figure 1). The pH dynamics could be systematically controlled by varying the concentrations and types of enzymes and substrates. Notably, this behavior emerged autonomously without any additional physicochemical operations, despite the system being completely closed. Furthermore, we developed a numerical model to elucidate the mechanism underlying the observed pH dynamics. Finally, the pH-regulating system was applied as a controlling element to modulate pH-responsive molecular self-assembly processes and the pH waveforms inside giant–unilamellar–vesicles, including micelle–vesicle and sol–gel transitions, demonstrating its potential applicability in smart material design.

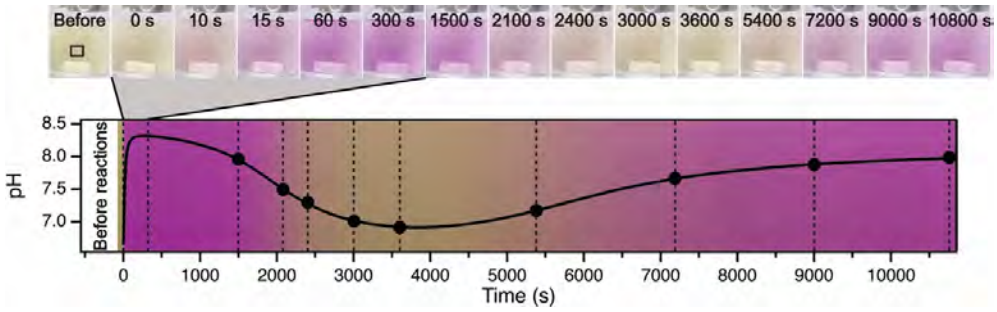

Figure 1. Obtained autonomously recursive pH dynamics in a batch reactor, where pH is indicated by phenol red (snapshots of the reactor at upper part), and the measured pH is plotted with the color change (lower part). Experiments were carried out with [ethyl acetate] = 30 mM, [urea] = 10 mM, [esterase] = 0.4 U/mL, [urease] = 1.0 U/mL, [KCl] = 100 mM , and T = 25±0.5˚C.

Monitoring of diffusion-controlled acid-base reaction in agarose gel matrix and its possible applications

Norbert Német[1], **Stevan Maćešić**[2], **Gábor Schuszter**[3], **István Lagzi**[1,4]

[1]Budapest University of Technology and Economics, Department of Physics, Budapest, Hungary
[2]University of Belgrade, Faculty of Physical Chemistry, Belgrade, Serbia
[3]University of Szeged, Department of Physical Chemistry and Materials Science, Szeged, Hungary
[4]ELKH-BME, Condensed Matter Research Group, Budapest, Hungary

Most chemical waves and fronts produced by diffusion-driven reactions in solid hydrogels are unidirectional (e.g., Liesegang pattern formation [1] or Belousov-Zhabotinsky-waves[2]). In our systems, as a simple solid phase acid-base neutralization reaction, the chemical front is a retreating boundary in space and time. The base is homogeneously dispersed in an agarose hydrogel, while the acid solution serves as the outer electrolyte. Based on the ratio of acid to base and gel column, the system will reach beyond the equivalence point through pure diffusion. In this setup, hydrodynamic convection can be excluded, leaving only the simple liquid phase, so the acid-base boundary is clearly visible in the presence of an indicator dye. [3]

In our setup, we dispersed sodium hydroxide base in agarose gel poured into vials in a given amount and placed different concentrated acid solutions on the gel surface as outer electrolyte (V_{gel}=2.5×V_{acid}). Both phases contain methyl red pH dye as a sensor to detect the pH change during the process (**Fig. 1, a**). The acid-base (red-yellow) boundary was followed by an image processing system for three days, and the photographs were analyzed to detect the front position. In a given acid concentration, the front reached a semi-stable state, from which it later reversed because of the local acid reduction in the gel's upper segment and the diffusion of hydroxide ions from the gel's lower segment.

We have been searching for possible applications to exploit the circumstances of this phenomenon. One possible way is the pH-dependent, diffusion-controlled crystal engineering. Zeolitic imidazolate frameworks (ZIFs) are a subset of metal-organic frameworks (MOFs), which are organic-inorganic hybrid porous compounds with high surface area and thermal stability.[4] ZIFs can be synthesized in a neutral pH environment, but under acid conditions, they decompose. We used ZIF-14 in our system, which contains zinc cation metal nodes connected by 2-ethylimidazole organic linker bridges. Slow diffusion and time and space-dependent pH conditions influence nucleation, crystal growth, and ultimately the morphology and particle size of the crystals (**Fig. 1, b**).

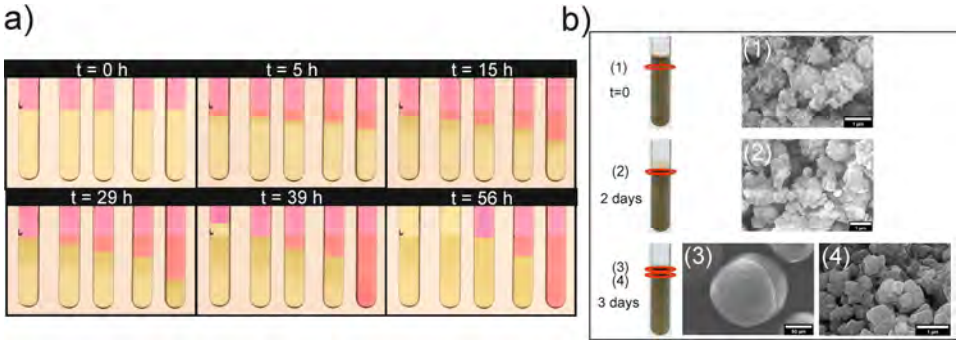

Fig. 1 a) Capture photos of acid-base reaction diffusion front movement. Gel content: $[NaOH]_0$ = 0.5 M, $[Methyl\ red]_0$ = 20 mM, 1% agarose gel with 4 cm height in 1 cm inner diameter glass vials. Outer electrolyte acid solutions from left to right: $[HCl]_0$ = 0.6 M; 0.7 M; 0.8 M; 0.9 M; 1.5 M, $[Methyl\ red]_0$ = 20 mM, V_{acid}=1.5 mL.
b) Scanning electron micrographs of ZIF-14 particles extracted from agarose segments. Gel content: $[NaOH]_0$ = 0.5 M, $[ZIF\text{-}14]_0$ = 30 mM, 1% agarose gel with 4 cm height in 1 cm inner diameter glass vials. Outer electrolyte acid solution: $[HCl]_0$ = 0.9 M; $[Zn^{2+}]_0$ = 30 mM; $[2\text{-}ethylimidazole]_0$ = 300 mM, V_{acid}=1.5 mL.

We also investigated inorganic hydroxide precipitations and gold nanoparticles' aggregation, and oleic acid micelle-vesicle systems.

Synthesis of crystalline materials from macro- to microscale

István Lagzi[1,2]

[1] Department of Physics, Institute of Physics, Budapest University of Technology and Economics, H-1111 Budapest, Hungary
[2] HUN-REN−BME Condensed Matter Physics Research Group, Budapest University of Technology and Economics, H-1111 Budapest, Hungary

Diffusion-assisted synthesis in rigid gel matrices offers a powerful route to controlling crystallization through reaction–diffusion processes. In this talk, we present gel-based fabrication strategies for producing crystalline materials with tunable size, morphology, and dispersity. Using gel columns, flow-through gel reactors, and reactive wet stamping, we demonstrate the synthesis of diverse material classes, including inorganic precipitates, metal–organic frameworks, and gold nanoparticles. In these systems, reactants are initially spatially separated; crystal formation occurs as one reagent diffuses into a gel containing the other, yielding crystals whose sizes increase linearly with distance from the gel interface. The gel matrix suppresses sedimentation and aggregation, enabling undisturbed growth of larger crystals, while providing spatiotemporal control over reagent flux, nucleation, and growth kinetics. The observed linear size gradients are captured by theoretical models that link larger crystal sizes to regions of lower supersaturation, where growth dominates over nucleation. We further discuss advanced approaches—such as orthogonal diffusion and electric field-assisted synthesis—that extend spatial control and enable complex crystal morphologies. Compared to conventional bulk wet synthesis, diffusion-assisted methods afford exceptional precision in crystal size and shape. Finally, we outline prospects for scaling macroscopic crystal growth, developing 2D and 3D reactor architectures, and translating these techniques to applications in catalysis, biomedicine, and environmental remediation.

Acknowledgements
This research was supported by the HUN-REN Hungarian Research Network, the National Research, Development and Innovation Office of Hungary (K146071), the Ministry of Culture and Innovation, and the National Research, Development and Innovation Office under Grant No. TKP2021-EGA-02.

References

1. Norbert Német, Gabor Hollo, Sung Ho Yang, Bilge Baytekin, Gabor Schuszter, Istvan Szalai, Federico Rossi, Istvan Lagzi: “Diffusion-assisted synthesis of crystalline materials in rigid gels”, CrystEngComm, 10.1039/D5CE00589B

Day 2
24 Jan., 2026 (Sat)

Dimensional Fate of Traveling Waves in Active Polar Media

From One-Dimensional Waves to Two-Dimensional Defect Dynamics

Min-Jhe Lu[1] and Shunsuke Yabunaka[2]

[1]Institute of Computational and Modeling Science, National Tsing Hua University, Hsinchu, Taiwan
[2]Advanced Science Research Center, Japan Atomic Energy Agency, Tokai, Japan

Traveling waves are a characteristic feature of active polar systems, observed both in theoretical models and in experiments on cohesive tissues, and are commonly interpreted through linear stability analyses.

An important open question is whether traveling waves can persist as asymptotic dynamical attractors in active polar media once transverse degrees of freedom and topological defects are permitted.

In this work, we address this question by comparing one- and two-dimensional active polar models within a unified theoretical and numerical framework. In one dimension, traveling waves arise robustly and are well characterized by their selected wavelength and propagation speed. We further refine the linear diagnostics by examining mode structure and transient responses, which reveal regimes that are linearly stable yet highly responsive to perturbations.

In two dimensions, instead, depending on initial conditions and activity strength, the system relaxes into one of two statistically steady states: an ordered but non-propagating configuration, or a defect-rich active turbulent state. Using steady-state diagnostics based on kymographs and cross-correlation drift measurements, we demonstrate that apparent local motion in two dimensions does not correspond to net wave propagation. This raises the question of whether the traveling-wave solutions identified in one dimension persist in two dimensions as stable or metastable states, and how their stability properties are altered by transverse modes and defect dynamics.

Together, these results clarify how dimensionality and defect dynamics fundamentally reshape traveling-wave behavior in active polar media.

Acknowledgements

Part of this work was developed during the NCTS Research in Pairs program in Taiwan, December 2025.

References

Serra-Picamal, Xavier, et al. “Mechanical waves during tissue expansion,” *Nature Physics* **8**. 8 (2012): 628-634.

S. Yabunaka and P. Marcq, “Cell growth, division, and death in cohesive tissues,” *Phys. Rev. E* **96**, 022406 (2017). DOI: 10.1103/PhysRevE.96.022406

A Higher-Order Vicsek Model Emerging from Local Conformity

Keisuke Taga[1,2], Riccardo Muolo[2,3], Hiroya Nakao[2,4], and Iván León[5]

[1] Department of Physics and Astronomy, Tokyo University of Science, Japan
[2] Department of Systems and Control Engineering, Institute of Science Tokyo (former Tokyo Tech), Japan
[3] RIKEN Center for Interdisciplinary Theoretical and Mathematical Sciences (iTHEMS), Japan
[4] International Research Frontiers Initiative, Institute of Science Tokyo (former Tokyo Tech), Japan
[5] Department of Applied Mathematics and Computer Science, Universidad de Cantabria, Spain

Simple interactions among a large number of individuals can generate rich spatiotemporal patterns, such as the flocking observed in birds, fish, and bacteria. The Vicsek-type alignment model [1,2] is one of the fundamental formulations, in which the position x_j and heading θ_j of particle j evolve as

$$\dot{\boldsymbol{x}}_j = \boldsymbol{v}_j, \qquad \boldsymbol{v}_j = v_0(\cos\theta_j, \sin\theta_j),$$
$$\dot{\theta}_j = \frac{1}{n_j}\sum_{k\sim j} w_{jk}\sin(\theta_k - \theta_j) + \eta\,\xi_j(t),$$

where $k \sim j$ denotes neighbors within the interaction range r_0, n_j is the number of neighbors, and $\xi_j(t)$ is Gaussian white noise with intensity η. w_{jk} denotes the interaction weight from k to j; we propose a new form to represent local conformity.

Recently, there has been a growing interest towards higher-order interactions [3,4,5], because they can induce collective behaviors that cannot arise from pairwise interactions alone. In this study, we show that *local conformity* naturally generates higher-order interactions in flocking dynamics [6]. Conformity means that an individual preferentially follows neighbors aligned with the local majority direction, assigning smaller influence to neighbors oriented against it. We implement this mechanism by introducing the conformity-based weights

$$w_{jk} = a + \frac{b}{n_j}\sum_{l\sim j}\cos(\theta_l - \theta_k),$$

Substituting this weight into the Vicsek-type alignment rule, it yields an equivalent model with explicit three-body interactions:

$$\dot{\theta}_j = \frac{\alpha}{n_j}\sum_{k\sim j}\sin(\theta_k - \theta_j) + \frac{\beta}{n_j^2}\sum_{k,l\sim j}\sin(2\theta_k - \theta_l - \theta_j) + \eta\,\xi_j(t), \qquad \alpha = a - \frac{b}{2},\ \beta = \frac{b}{2}.$$

We demonstrate that the model exhibits multiple collective regimes, including coherent order, disorder, and a bidirectionally ordered state (particles moving in opposite directions) in the deterministic case. We also investigate the noisy case, where the system undergoes continuous and discontinuous order--disorder phase transitions, and discuss the stability of each collective state. The transition belongs to a different universality class which, to our knowledge, has not been reported in the existing Vicsek-type alignment models.

References

1. T. Vicsek and A. Zafeiris, “Collective motion”, Phys. Rep. 517, 71 (2012).
2. H. Chaté, “Dry aligning dilute active matter”, Ann. Rev. of Cond. Matt. Phys. 11, 189 (2020).
3. P. Skardal and A. Arenas, “Higher order interactions in complex networks of phase oscillators promote abrupt synchronization switching”, Comm. Phys. 3, 1 (2020).
4. I. León, R. Muolo, S. Hata, and H. Nakao, “Higher-order interactions induce anomalous transitions to synchrony”, Chaos 34, 013105 (2023).
5. I. León, R. Muolo, S. Hata, and H. Nakao, “Theory of phase reduction from hypergraphs to simplicial complexes: a general route to higher-order Kuramoto models”, Physica D 482, 134858 (2025).
6. I. León, R. Muolo, H, Nakao and K. Taga, “Collective dynamics of higher-order Vicsek model emerging from local conformity interactions”, in preparation.

Emergent Collective Dynamics of Active Polar Particles in Heterogeneous Aligning Fields

Chung Wing Chan[1], Marie Tani[1], Masatoshi Ichikawa[1,2], Ibuki Kawamata[1], Akira Kakugo[1]

[1]Division of Physics and Astronomy, Graduate School of Science, Kyoto University, [2] Graduate School of Integrated Science for Life, Hiroshima University.

Introduction

Active matter consists of self-propelled agents that convert environmental energy into motion, leading to emergent collective behaviors such as swarming via local alignment interactions. These phenomena have been widely studied using particle-based models, notably the Vicsek model, and coarse-grained hydrodynamic theories such as the Toner–Tu equations. Experimentally, collective motion occurs in diverse systems, from bacterial colonies and neuronal cells to artificial active materials including Janus particles and kinesin–microtubule assemblies[1]. Notably, while biological active matter typically operates in intrinsically spatially heterogeneous environments, most theoretical models and artificial experimental realizations assume homogeneous alignment fields for simplicity. This mismatch limits our understanding of how environmental heterogeneity influences collective dynamics, leaving the behavior of active polar particles in spatially heterogeneous alignment fields largely unexplored.

Results

In this study, we extend the Vicsek model by introducing a spatially dependent alignment field and derive a corresponding coarse-grained hydrodynamic theory. All coefficients are explicitly derived from microscopic parameters, enabling a direct one-to-one comparison between simulations and continuum descriptions. We show that the geometry of the alignment field can shape the direction of swarming and identify a novel spatiotemporal oscillatory swarming mode that emerges in striped pattern of alignment field (Fig. 1). The continuum theory accurately reproduces key features observed in simulations and offering a computationally efficient framework for exploring complex alignment field landscapes. It enable analytical insights, in particular, we analytically demonstrate the linear stability of biased swarming states in striped fields. Experimentally, we develop a photo-responsive kinesin–microtubule gliding assay using UV-sensitive DNA, in which DNA-modified microtubules are propelled by kinesin motors and their alignment interactions are controlled by spatially patterned ultraviolet light[2]. This experimental platform allows us to validate our theoretical predictions and offers general design principles for adaptive active materials and swarm robotic systems responsive to external cues.

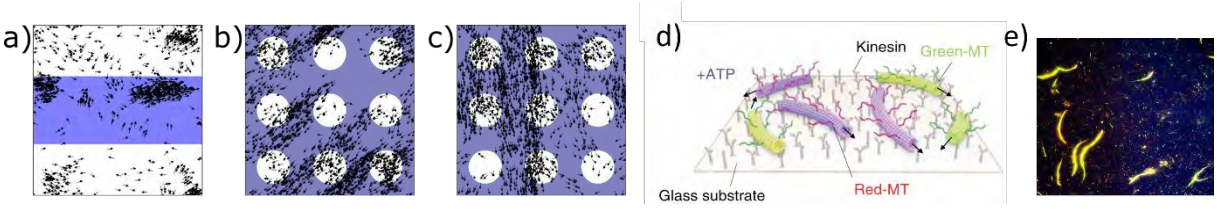

Fig. 1 (a-c) Snapshort of simulation. (d)Schematic of the experimental setup (e) Expermental image of MTs swarming.

Acknowledgement

This work was supported by JST SPRING, Grant Number JPMJSP2110.

Reference

1. Vicsek. & Zafeiris, Collective motion. *Physics reports*, *517*(3-4)(2012).
2. M. Akter *et al.,* Cooperative cargo transportation by a swarm of molecular machines, *Sci. Robot.***7**,eabm0677(2022).

Translational motion of droplet cluster under oscillatory shear

Tsubasa Yoneda[1], **Takuya Ohmura**[2], **Yukinori Nishigami**[2], **Hiroshi Orihara**[2], **Toshiyuki Nakagaki**[2]

[1] Graduate school of Life Science, Hokkaido University, Sapporo, Japan
[2] Research Institute for Electronic Science, Hokkaido University, Sapporo, Japan

Soft interfaces, such as those of bubbles, droplets, and cells, exhibit diverse dynamics coupled with surrounding fluids. Under shear flow in confined environment, hydrodynamic interactions often drive these objects to self-organize into ordered structures[1][2]. Here we examined the behavior of oil-in-water droplet emulsion (diameter: 8~20 μm) under tight confinement and symmetric oscillatory shear (Fig a). We found spontaneous aggregation of the droplets, where the resulting clusters includes 2 to 10 polydisperse droplets. Moreover, in contrast to the simple back-and-forth motion of the single droplets following the symmetric oscillatory displacement of the shearing plate, some droplet clusters showed translational motion along the direction of shear (x-axis) (Fig. b). The translational motion lasted over spatiotemporal scale (amplitude and period) of oscillatory shear, and had no apparent bias in the direction of the motion (positive or negative in x-axis). Thus, we consider that the translational motions of droplet clusters were spontaneously breaking the symmetry of mechanical input.

To simply capture a key factor for driving clusters and determining the direction of motion, we focused on two-droplet clusters. The sign matching between droplet diameter difference in clusters (positive when the right droplet is larger) and x-axis velocity (positive when the cluster moves to the right) clearly showed the principle determining the direction: the larger droplet leads the motion. The experimental results represent that droplet size anisotropy within a cluster enables itself to move asymmetrically.

The flow field around the single droplet under the oscillatory shear was like a quadrupole, which flow speed depended on the cube of droplet radius. As discussed in previous studies[2], such quadrupole-like flow from a droplet can attract surrounding droplets along the shear direction, whereas a droplet cannot propel itself via its own flow field. We numerically calculated the motions of two droplets with the hydrodynamic interaction and the excluded volume effect as a physical contact force, which successfully reproduced the attraction of droplets and the formation of steady clusters. Moreover, the two-droplet cluster in the simulation was driven by a net force into the direction consistent with the experiment (Fig. c). From the numerical results, we propose a two-step view of the moving mechanism; (1) every single droplet generates quadrupolar flow through interface dynamics (2) non-reciprocal inter-droplet hydrodynamic interaction realizes clustering and motion.

To investigate material dependence of the translational motion under the confined oscillatory shear, we performed experiments with other materials. Interestingly, the translational motions were observed not only in droplet emulsions but also in a variety of micrometer-scale materials, such as aggregated colloidal beads, amoeba cell fractions and passive carcasses of small multicellular organisms. The independence of material highlights potential applications, such as micro-robots and drug delivery system. We believe that our investigation on the droplet would provide the simplest model system to reveal its fundamental mechanism.

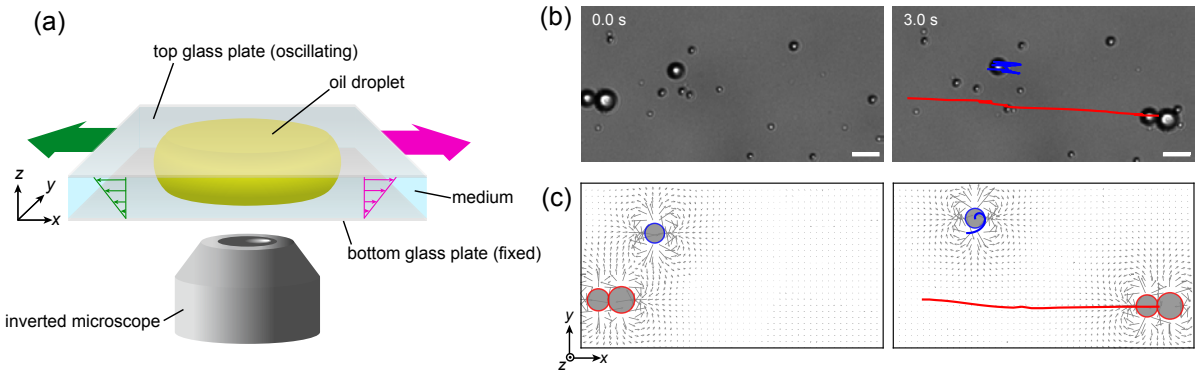

Figure : (a) The experimental setup. (b) Simple back-and-forth motion of droplet (blue line) and translational motion of two-droplet cluster (red line). (c) Numerical calculation of droplet motion.

References

1. Z. Shen, T. M. Fischer, A. Farutin, P. M. Vlahovska, J. Harting, and C. Misbah, Blood Crystal: Emergent Order of Red Blood Cells Under Wall-Confined Shear Flow, Phys. Rev. Lett. **120**, 268102 (2018)..
2. S. Singha, A. R. Malipeddi, M. Zurita-Gotor, K. Sarkar, K. Shen, M. Loewenberg, K. B. Migler, and J. Blawzdziewicz, Mechanisms of spontaneous chain formation and subsequent microstructural evolution in shear-driven strongly confined drop monolayers, Soft Matter 15, 4873 (2019).

Active particle in a thin interfacial droplet

Airi N. Kato[1], **Kaili Xie**[1,2], **Benjamin Gorin**[1], **Jean-Michel Rampnoux**[1], **Hamid Kellay**[1]

[1]Laboratoire Ondes et Matière d'Aquitaine (LOMA), Université de Bordeaux, Bordeaux, France
[2]Van der Waals-Zeeman Institute, Institute of Physics, University of Amsterdam, Amsterdam, the Netherlands

Confinements, which make active particle dynamics distinct from that in bulk, are ubiquitous in most experimental systems. Soft boundaries, such as droplet interfaces, are deformable confinements for active particles. However, the physical mechanisms underlying the interplay between activity and interfacial effects remain poorly understood, particularly in simpler quasi-two-dimensional systems. This work focuses on this point using an active particle in a thin film droplet. We utilized a light-driven Janus particle in a surfactant-free thin oil droplet, stabilized at an air–water interface.

We found that the active particle motion strongly couples with the droplet thickness profile changes. The particle is driven by a thermal Marangoni flow [1] at 1mm/s–1cm/s. In addition, the particle exhibits various motions, from periodic circular motions (Figure 1(a)) to intermittent irregular motions. We found that this variety originated from the confinement by the droplet. By taking capillarity into account [2], we clarified that the periodic circular motions arise from the interplay of activity, a capillary centripetal force due to the lens-like droplet geometry, and a capillary torque due to the non-equilibrium interfacial profile [3].

If time allows, we will also show some preliminary results from an extended project on a much softer interfacial droplet with surfactants. Unlike in surfactant-free cases, the droplet is not simply confining the particle; it exhibits net propulsion (Figure 1(b)) at O(10um/s). Large contact-line deformations are observed in addition to changes in the thickness profile, driven by the particle motion.

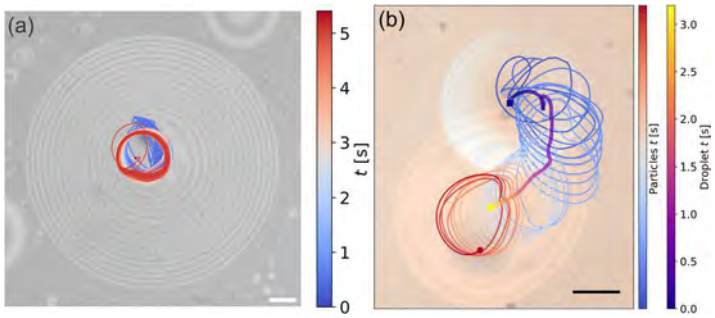

Fig. 1 ： (a) Trajectory of a circular motion of a Janus particle in surfactant-free thin droplets. (b) Trajectory of the particle motion and droplet net motion. Initial and final droplets are superimposed in the image. Scalebar=50um.

Acknowledgements

We thank T. Bickel, Y. Tagawa, and K. A. Takeuchi for helpful and interesting discussions. We are particularly indebted to A. Würger for numerous discussions.

References

1. K. Dietrich, N. Jaensson, I. Buttinoni, G. Volpe, and L. Isa, *Phys. Rev. Lett.* **125**, 098001 (2020).
2. A. Yadav, E. J. Hinch, and M. S. Tirumkudulu, *Phys. Rev. Lett.* **122**, 098001 (2019).
3. A. N. Kato, K. Xie, B. Gorin, J-M. Rampnoux, and H. Kellay, *Phys. Rev. Research* **7**, L042023 (2025).

Collective Phenomena of Active Particles Communicating through Diffusion Fields

Keita Fujita, Hiroyoshi Nakano, and Hiroshi Noguchi

Institute for Solid State Physics, University of Tokyo, Kashiwanoha, Chiba, Japan

The collective behaviors of self-propelled agents, from bacteria to animal groups, are a central focus in active matter physics. While established models like the Vicsek and active Brownian particle models have elucidated the roles of self-propulsion, local alignment, and disorientation in creating active matter's cooperative phenomena, the influence of chemical signaling (chemotaxis) remains relatively underexplored [1]. In colonies of chemotactic bacteria, such as Escherichia coli and Salmonella typhimurium, individual agents actively modify their environments by releasing chemical substances and subsequently adjust their behaviors in response to emergent chemical gradients. Consequently, these agents engage in indirect interactions through self-generated chemical landscapes. Unraveling how these chemically mediated interactions give rise to complex cooperative phenomena and how these phenomena manifest in living systems represents a crucial frontier.

Motivated by this, we developed a simplified model of self-propelled particles interacting through a diffusive chemical field. Our model consists of self-propelled particles and a chemical substance, represented as a continuum field $u(\boldsymbol{r}, t)$. The chemical field evolves according to a diffusion equation, while the particles' motion is governed by Newton's equations with two primary forces: a constant self-propulsion force v_0 and a chemotactic force that drives them towards regions of lower chemical concentration.

Analyzing this model, we observe three distinct phases dependent on self-propulsion magnitude and particle density, as depicted in Fig. 1. Figure 1(a) presents a disordered phase, characterized by the absence of any long-range order. Figure 1(b) shows a hexagonally ordered phase, characterized by particles forming a crystalline-like arrangement. This phase emerges with increased particle density or decreased self-propulsion. Finally, Fig. 1(c) presents a traveling square pattern phase, where both particles and the chemical field form a coherently moving square lattice. In our presentation, we will discuss the properties of these distinct phases and their potential relevance to living systems.

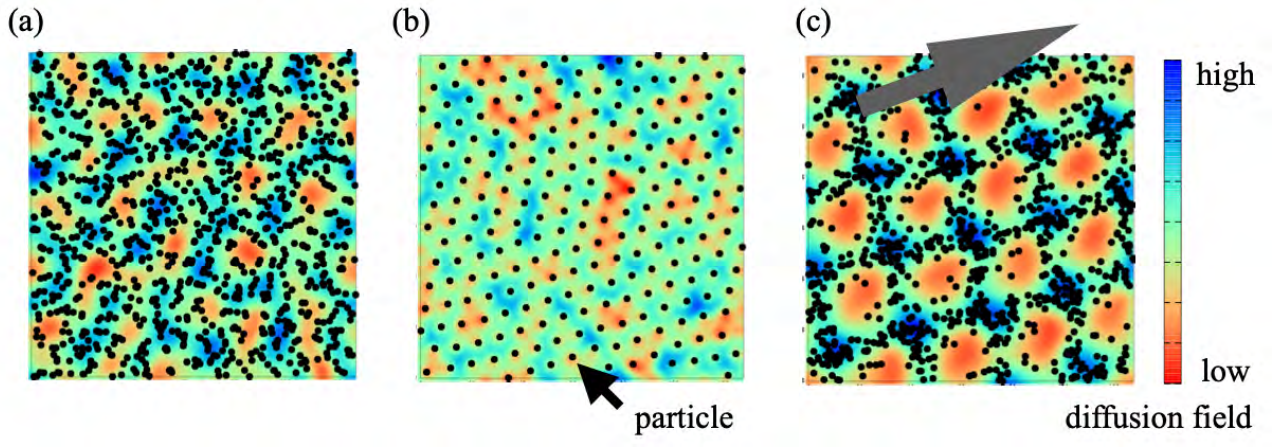

Fig. 1 Typical snapshot of three phases appearing in our model. (a) disordered phase. (b) hexagonally ordered phase. (c) traveling square pattern phase. In all figures, black points represent self-propelled particles, and the background color indicates the magnitude of the diffusion field.

References

1. A. Ziepke, I. Maryshev, I. S. Aranson, and E. Frey: "Multi-scale organization in communicating active matter", Nat. Commun. **13**, 6727 (2022).

Spatiotemporal Patterns in Active Potts Models

Hiroshi Noguchi

Institute for Solid State Physics, University of Tokyo, Kashiwa, Chiba, Japan

We studied the effects of thermal fluctuations on pattern formation using MC simulations of active Potts models [1-7]. The Potts model is extended to have an energy consumption in cyclic flip loops of states. It is a model system for chemical reactions on a catalytic surface or molecular transport through a membrane.

I will focus on the cyclically symmetric condition in this presentation. At low flip energies, single-state-dominant phases cyclically change through nucleation and growth (homogeneous cycling mode). In contrast, spiral or non-spiral waves are formed at high flip energies. In particular, when factorizable numbers of states are used, spatiotemporal patterns with factorized symmetry emerge [5]. For example, in the six-state Potts models, spiral waves with three domain types (one state dominant or two states mixed), three-state mixed phases, and three-state homogeneous cycling are formed in addition to the six-state wave and homogeneous cycling modes, as shown in Fig. 1. Although three states can coexist spatially under thermal equilibrium, the scaling exponents of the transitions to the wave modes are modified from the equilibrium values.

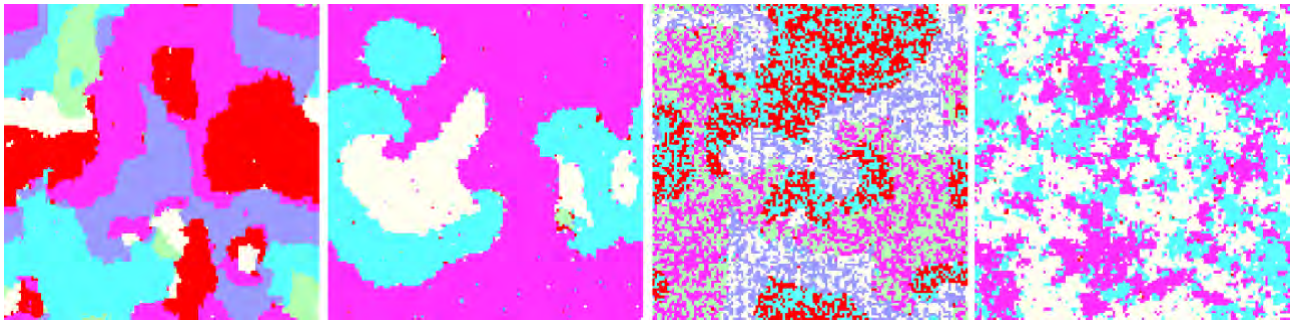

Fig. 1 ： Snapshots of the six-state Potts model. Six-state wave (W6), three-state wave (W3), wave of mixed states (M2W3), and three-state mixed phase (M3), from left to right.

References

1. H. Noguchi, F. van Wijland, and J.-B. Fournier, *J. Chem. Phys.* **161**, 025101 (2024).
2. H. Noguchi and J.-B. Fournier, *New J. Phys.* **26**, 093043 (2024).
3. H. Noguchi, *Soft Matter* **21**, 1113 (2025).
4. H. Noguchi, *Sci. Rep.* **15**, 674 (2025).
5. H. Noguchi, *Phys. Rev. Res.* **7**, 033243 (2025).
6. H. Noguchi, arXiv:2509.17408.
7. H. Noguchi, arXiv:2512.01394.

The Spatial Structure of Horse Social Groups

Tamao Maeda[1], **Monamie Ringhofer**[2], **Sota Inoue**[3,4], **Satoshi Hirata**[5], **Shinya Yamamoto**[6]

[1] Research Center for Integrative Evolutionary Science, The Graduate University for Advanced Studies (SOKENDAI), Kanagawa, Japan
[2] Faculty of Life and Environmental Sciences, Department of Animal Sciences, Teikyo University of Science, Yamanashi, Japan
[3] Institute for Advanced Research, Nagoya University, Aich, Japan
[4] Graduate School for Environmental Studies, Nagoya University, Aich, Japan
[5] Wildlife Research Center, Kyoto University, Kyoto, Japan
[6] Institute for the Future of Human Society, Kyoto University, Kyoto, Japan

Spatial organisation in animal groups has long been a focus of research, and numerous modelling studies, such as Boid model and Vicsek model, have explored the dynamics arising from local interaction rules. Classical approaches typically treated animals as homogeneous, particle-like entities without individuality or social relationships. More recent work, however, has begun to incorporate more biologically realistic features, such as visual fields, social interactions, and individual differences, and has shown that these factors can substantially improve the ability of models to reproduce group-level functions and properties [1–3]. Despite this progress, empirical studies of collective spatial structure remain heavily biased towards taxa that can be readily observed under captive or highly controlled conditions. In particular, it has been difficult to obtain quantitative data on large mammals.

In this study, we focus on feral horses, which exhibit complex social organization, and provide a comprehensive description of their group-level spatial structure in the wild condition. Horses form multilevel societies in which stable and small social group (“units”) aggregate to form higher-level groups [4]. To quantify the spatial structure of a multilevel horse society comprising more than 100 individuals, we developed a drone-based observation method that allowed us to obtain high-resolution spatial snapshots of entire aggregations.

Our observations revealed a highly heterogeneous spatial structure: small distances within units and larger distance between units (Fig1). Inter-individual distances within units were typically around 2–3 m, whereas inter-unit inter-individual distances were around 50 m [4]. A more detailed analysis of the mechanisms underlying this structure suggested that different units maintained distances that were neither too close nor too far from one another. Randomization analyses showed that units tended to avoid very close inter-unit proximity (0–14 m) and situations in which individuals from different units became intermixed. At the same time, observed inter-unit distances were shorter than those expected from randomized data, and neighboring units displayed synchronized behavior [5]. These patterns indicate that units actively aggregate to form larger groups while maintaining spatial segregation.

We presume that this spatial structure reflects a balance between the benefits of aggregating with other units and the need to minimise inter-unit conflict. In equines, multiunit aggregation is suggested to occur because of decreased predation pressure [6], increased efficiency in finding shelters [7], and reduced harassment from bachelors [8]. In contrast, unit males are reproductively competitive. Males exhibit defensive and aggressive behaviour when rival males approach their units [9,10]. Such inter-male competition and male behaviour for unit maintenance are essential for the formation of a horse multilevel society. Our results imply that the trade-off between inter-unit competition and the benefits of forming larger aggregations is expressed in the moment-to-moment spatial structuring of multilevel groups.

Acknowledgements
We would like to give a special thanks to Viana do Castelo City for supporting our project. We are grateful to Renata Mendonça, Pandora Pinto, Cédric Sueur, and Sebastian Sosa for their support throughout the study. We thank the residents of Montaria for their assistance during our stay, as well as Sakiho Ochi and the volunteers that contributed to data collection during the field work.

Swarming in 1-dimension: an empirical and numerical study on Iriomote-native soldier crabs

Claudio Feliciani[1], **Riccardo Muolo**[2,3] , **Hisashi Murakami**[4], **Sakurako Tanida**[1], **Hiroya Nakao**[3]

[1]Department of Aeronautics, The University of Tokyo, Japan
[2]iTHEMS, RIKEN, Japan
[3]Department of Systems and Control Engineering, Institute of Science Tokyo, Japan
[4]Faculty of Information and Human Science, Kyoto Institute of Technology, Japan

Swarming behavior is common in many animal groups, such as fish, insects, and crabs. Several studies considered the motion of animal groups through field observations or laboratory experiments. However, the bi or tri-dimensional motion of swarms made numerical modeling a difficult task, with most models aimed at reproducing qualitative features found in nature (such as milling, flocking, etc.). This work investigates swarming behavior in soldier crabs from Iriomote island (Okinawa), which provide a particularly suitable system for empirical study, as they naturally form dense, cohesive swarms with clear collective motion over extended periods [1]. Our experimental apparatus is a 1-dimensional domain with periodic boundary conditions, i.e., a circular track whose width is narrow enough to be modeled as a 1-dimensional domain, but large enough to allow crabs to move in opposite directions. The set up is depicted in Figure 1. The experiments have been carried out with 3, 10, and 30 crabs. Starting from the empirical observations, we analyze the trajectories and we characterize basic features of collective motion such as alignment, spacing, and response to local interactions. Building on those observation, we developed a data-driven 1-dimensional model of the crabs swarming behavior. We tuned the parameters of the model to part of the experimental data, to then validate them by comparing with further data. The 1-dimensional description allows us to extract essential features and interpolate settings with number of crabs between 3 and 30 on fine steps, for which the data is missing. Our model allows us not only to describe the setting observed in the experiments, but it is gives us a more general description of swarming in 1-dimensional domains, a very promising topic in active matter [2], that has not yet been thoroughly explored.

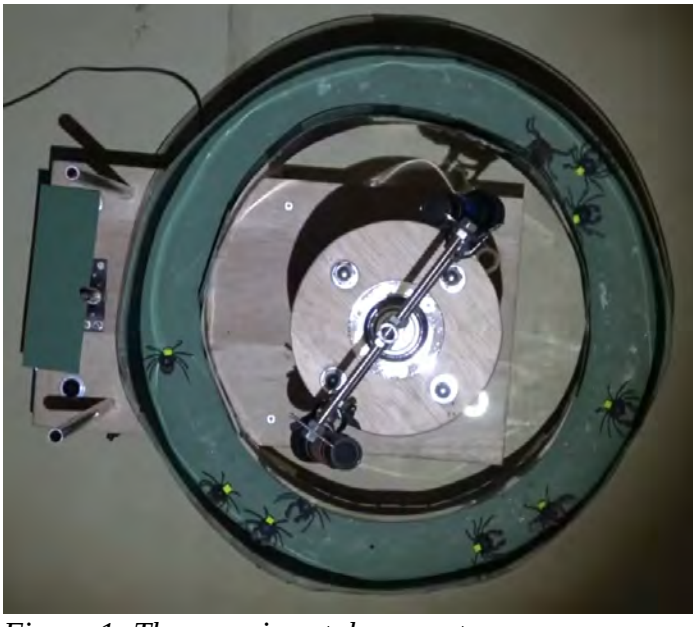

Figure 1: The experimental apparatus.

References

1. C. Feliciani, H. Murakami, T. Tomaru, Y. Uesugi, S. Tanida, Y. Nishiyama, X. Jia & T. Maeda: “How swarm size affects soldier crab swarming behavior: Laboratory experiments and ecological observations”, Artificial Life and Robotics 30, (Article 10.1007/s10015-025-01037-x) (2025).
2. B. Benvegnen, H. Chaté, P.L. Krapivsky, J. Tailleur, and A. Solon: “Flocking in one dimension: Asters and reversals”, Physical Review E 106, 054608 (2022).

Filamentous and dynamic raft structures in seabirds

Sota Inoue[1, 2, 3], Wataru Takeda[2], Shiho Koyama[2], Hibiki Sugiyama[2], Futoshi Ujiie[2], Kaho Minami[2], Chisaki Yashiki[2], Yusuke Goto[2], Ken Yoda[2]

[1]Institute for Advanced Research, Nagoya University
[2]Graduate School of Environmental Studies, Nagoya University
[3]Graduate School of Information Science and Technology, The University of Osaka

Seabird flocks often form massive aggregations at sea. Such strong attraction to conspecifics may operate not only within foraging flocks, but also during the formation of large rafts comprising thousands of individuals resting on the sea surface. It has been suggested that individuals preen and share information on foraging sites within these rafts. However, our understanding of rafts remains largely at the individual level, and collective-level phenomena have rarely been examined. To elucidate the mechanisms and adaptive significance of raft formation, close observation of rafts in situ is essential. In this study, we observed rafts of Streaked Shearwaters (Calonectris leucomelas) using drones around Awashima, Japan. It is empirically known that the birds form rafts before returning to their colony. We counted the number of individuals joining the rafts and reconstructed the two-dimensional shapes of the aggregations. In total, 264 rafts were identified, and the maximum raft size exceeded 20,000 individuals. The mean distance from the coastline to the rafts was 4,144 m. Two-dimensional reconstructions revealed filamentous formations that often extended over 1 km in length. Furthermore, we found that these filamentous formations were not created by drifting under the influence of wind or waves, but rather by the active movements of individuals. These findings suggest that seabird rafts are not static aggregations passively drifting at sea. Instead, they are dynamic structures in which individuals actively adjust their positions, likely following a set of behavioral rules that generate non-random spatial patterns.

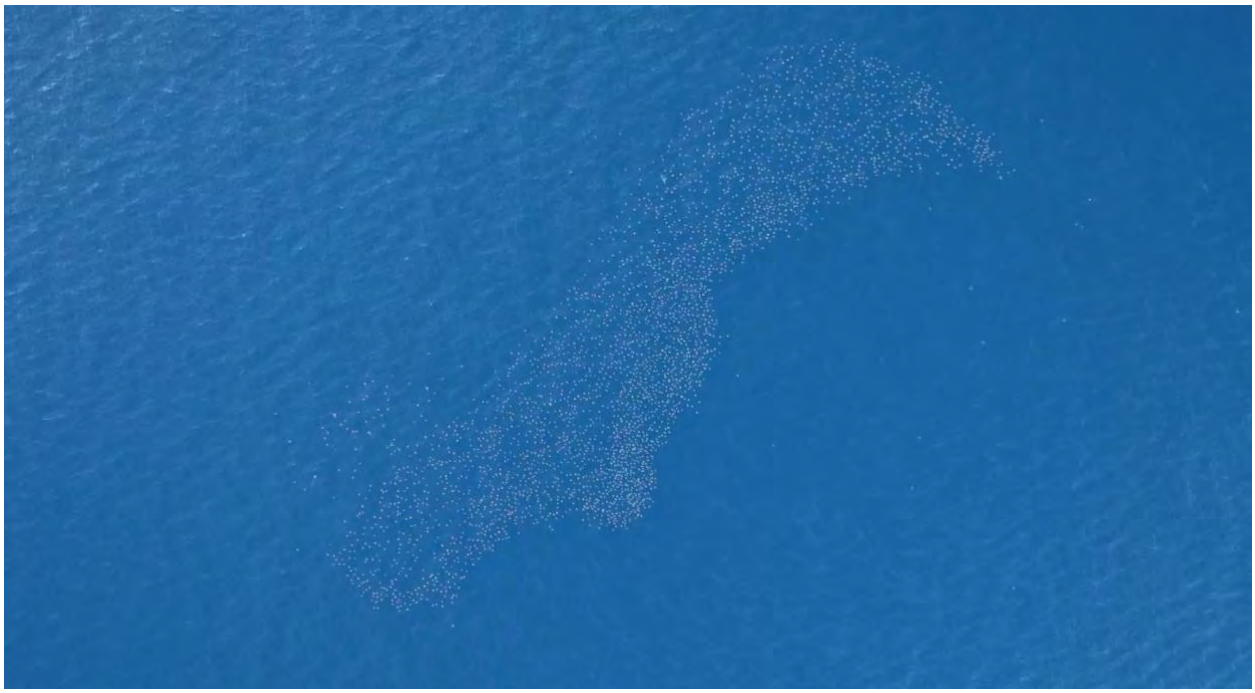

Fig. 1 ： An example of rafts of 3,000–4,000 Streaked Shearwaters.

Crowd management and active matter control in reality

Katsuhiro Nishinari

School of Engineering, University of Tokyo

Research on pedestrian dynamics has expanded rapidly in recent years, driven by advances in artificial intelligence and sensor technologies. Around the world, a wide range of studies have been conducted [1]—from high-precision crowd sensing to crowd behavior prediction through simulations, and even crowd control based on nudge theory. At the same time, public interest in safe and efficient crowd management, especially for large-scale events, has been steadily increasing.

Against this backdrop, we initiated research on crowd management with support from the government [2], collaborating with various stakeholders to develop data-driven approaches to crowd control. In this talk, I will present several real-world applications of our crowd management platform, including case studies at Tokyo Dome and JR Shinjuku Station. In these experiments, we successfully reduced congestion levels through the integrated use of sensing, simulation, and control technologies.

Fig.1: Tokyo Dome measurement by AI camera using Vorinoi diagram

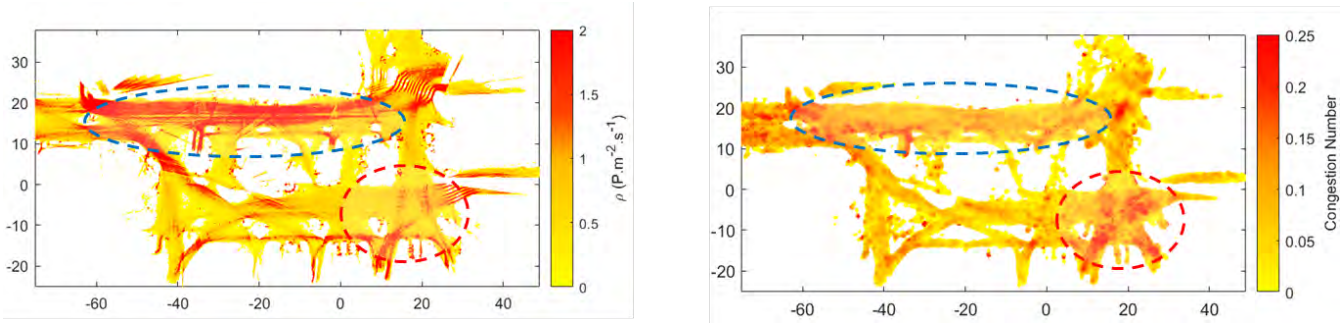

Fig.2: Visualization of congestion at JR Shinjuku station (left) by lidar sensors (right) by using a new congestion index[3].

Acknowledgements
This work was partially supported by JST-Mirai Program Grant Number JPMJMI20D1, Japan.

References

[1] C. Feliciani, et.al.,“Introduction to crowd management: Managing crowds in the digital era: Theory and practice,” Springer, 2022.
[2] K.Nishinari et. al., “Recent Developments in Crowd Management: Theory and Applications”, J. Disaster Res. vol.19, p.239, 2024
[3] C. Feliciani and K. Nishinari, “Measurement of congestion and intrinsic risk in pedestrian crowds”, Transportation Research Part C: Emerging Technologies, vol. 91, pp. 124–155, 2018.

Abstracts
for Poster presentations

Physical reservoir computing using the Vicsek model

Yuma Hida[1] and **Natsuhiko Yoshinaga**[1]

[1]Department of Complex and Intelligent Systems, Future University Hakodate,
Kamedanakano-cho 115-2, Hakodate 041-8655 Japan
(Dated: December 19, 2025)

Flocks are formed by some organisms, such as birds and fish. Despite differences among species, the flocks share common properties. One such property is that each individual aligns its orientation with that of its neighbors while in motion. Owing to this characteristic, a flock is able to behave as a coherent entity without a leader. Although individual agents exhibit fluctuations in their motion, the global structure of the flock responds flexibly to changes and perturbations from the external environment. Furthermore, flock structures may have acquired certain forms of efficiency through the process of evolution. For these reasons, it is promising to regard learning flocks as computational resources.

To utilize flocks as computational resources, we adopt the machine learning framework known as physical reservoir computing [1]. The motion of each individual in a flock exhibits complexity through its responses to external forces and possesses short-term memory as individuals gradually adjust their motion to that of their neighbors over time. These properties suggest that flocks can be naturally embedded as physical reservoirs. A number of studies have explored the use of various physical systems as reservoirs. Examples include a silicon arm robot that reproduces the dynamics of an octopus arm [1]. In the case of octopus-arm-based reservoirs, task-dependent strengths and weaknesses have been reported, providing insights into the relationship between information-processing structures and intelligence.

In this study, we employ a variant of the Vicsek model [2], a simple and general model of flocking. The input signal perturbs the orientation of each particle [3]. After measuring the orientation of each particle, we train the output data by optimizing the readout weights. Figure 1 shows the trajectory of particles' position calculated by the input-driven Vicsek model. The results of training are shown in Fig.2. With the trained weights, the dynamics of particles' orientation in Fig.1 predict well the NARMA10 task. Employing mathematical models of flocking for reservoir computing is meaningful in that it offers insights into intelligence at the collective level, where agents maintain orientational alignment while in motion, and is expected to reveal a simple form of collective intelligence.

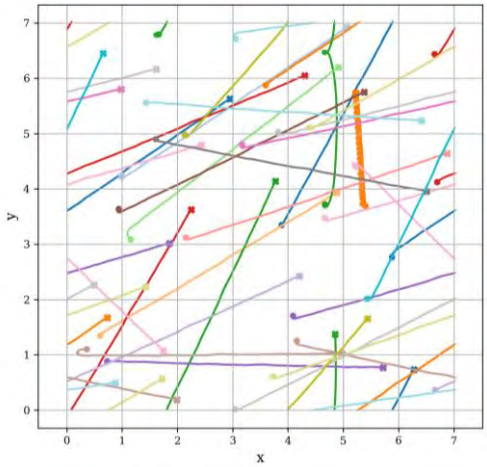

Fig.1: Trajectory of each particle under input.

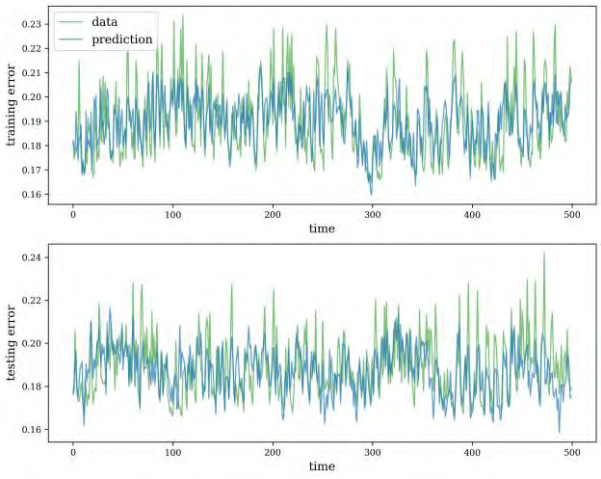

Fig.2: The training (top) and test (bottom) errors for the NARMA10 task using the Vicsek model.

References

1. Kohei Nakajima: "Physical reservoir computing—an introductory perspective", *Japanese J. Appl. Phys.* **59**, 060501 (2020).
2. Hugues Chaté: "Dry Aligning Dilute Active Matter", *Ann. Rev. Cond. Mat. Phys.* **11**, 189 (2020).
3. Thomas G. de Jong, Hirofumi Notsu, and Kohei Nakajima: "Harnessing omnipresent oscillator networks as computational resource", *arXiv:2502.04818* (2025).

Crystal stability of active matter

Takuma Hisamatsu[1]、**Duc T. Dam**[1]、**Yuta Kuroda**[2]、**Takesi Kawasaki**[3]、**Kunimasa Miyazaki**[1]
[1]Department of Physics, Nagoya University
[2]IV. Inst. Theor. Phys., Univ. Stuttgart
[3]D3 Center, Osaka University

Active matter systems are classified as nonequilibrium systems due to their self-propelling and are known to exhibit crystal stability distinct from that of equilibrium systems. For example, in the active Brownian particle (ABP) model, one of the simplest models, it has been theoretically predicted that in the limit of infinite persistence time ($\tau_p \to \infty$), long-range order is absent and crystals become unstable in dimensions $d \leq 4$ [1]. In contrast, in equilibrium systems, crystals are unstable only in dimensions $d \leq 2$. This implies that crystals in ABP systems are more prone to melting than in equilibrium systems. On the other hand, it has been shown that in chiral active Brownian particle (cABP) systems in the limit of infinite persistence time ($\tau_p \to \infty$), where rotational symmetry of motion is broken, crystals can remain stable even in dimensions $d = 2$ [1]. Thus, equilibrium, ABP, and cABP systems are expected to exhibit distinct crystal stability.

The equilibrium and ABP can be recovered from the cABP system by taking appropriate limits of the persistence time τ_p and the angular velocity Ω. Therefore, varying these parameters is expected to induce changes in crystal stability. In this study, we use numerical simulations to verify the predicted crystal stability and investigate how crystal stability evolves as the parameters are varied.

We performed molecular dynamics simulations in two-dimensional systems and calculated the mean squared displacement (MSD). The long-time limit of the MSD, denoted as A_L, is an indicator of crystal stability, and its behavior has been theoretically predicted for the three systems discussed above [1].

$$A_L \propto \begin{cases} \ln L & \text{(equilibrium)} \\ L^2 & \text{(ABP}(\tau_p \to \infty)\text{)} \\ const & \text{(cABP}(\tau_p \to \infty)\text{)} \end{cases} \tag{1}$$

Here, L represents the system size. Our simulation results show that, for parameter values corresponding to each system, A_L exhibits behavior consistent with the theoretical predictions. Furthermore, we find that the behavior of A_L changes across characteristic length scales given by $\xi_\Omega^X = 2\pi\sqrt{a_X/\Omega}$ and $\xi_{\tau_p}^X = 2\pi\sqrt{a_X\tau_p}$. These results demonstrate that the crystal stability is controlled by the interplay between the system size and the correlation lengths associated with the persistence time and the angular velocity.

Reference
[1]Y. Kuroda, T. Kawasaki and K. Miyazaki, Phys. Rev. Res., **7**(1), L012048 (2025).

How do topological defects of cell sheet reorient under external fluid flow?

Akito Saito[1], **Ryo Hanai**[1], **Daiki Nishiguchi**[1]

[1] Department of Physics, School of Science, Institute of Science Tokyo

Endothelial cells are responsible for the physiological function of angiogenesis. Elucidating the mechanism of angiogenesis from the perspective of active matter may provide novel methodology to the fields of bioengineering and biomaterials. Endothelial cells form a nematic structure with topological defects (Fig.1). A recent study suggests that half-integer topological defects are the sites where angiogenesis occurs [1]. Since vascular endothelial cells are exposed to shear flow induced by blood flow in vivo, the response of cells to shear flow has been investigated, and it is known that cells align in the direction of shear flow [2]. However, it remains unclear how the direction of topological defects and the surrounding velocity field respond under shear flow.

In our study, we investigated the external field response of topological defects in human umbilical vein endothelial cells (HUVECs) by applying shear flow. We observed tendency for +1/2 topological defect direction to align in the upstream direction and the average velocity field around defects qualitatively different from that in the absence of shear flow.

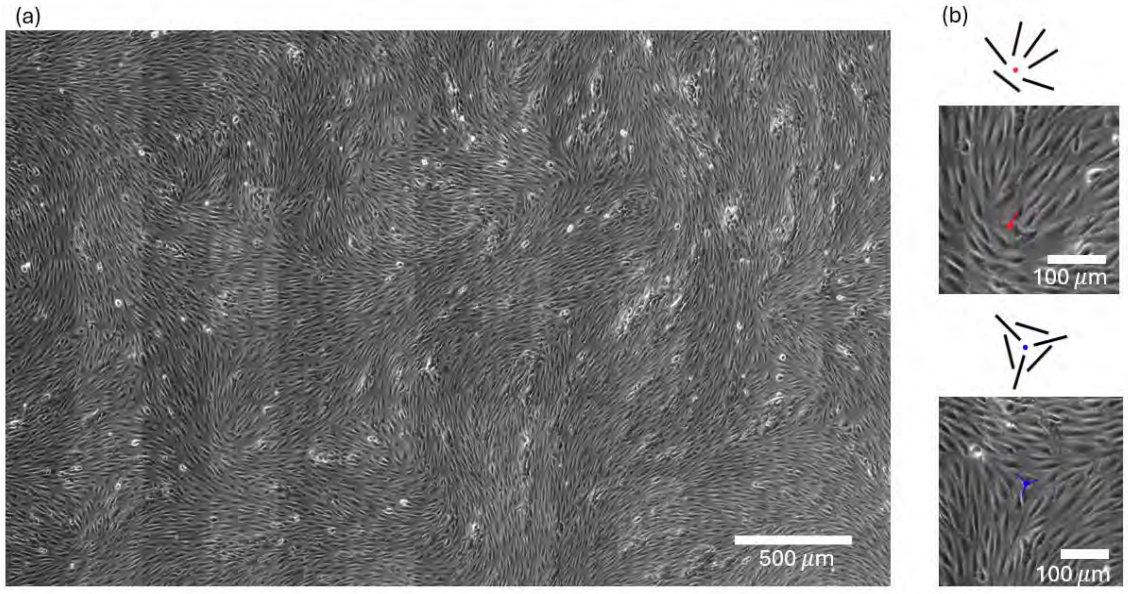

Fig. 1 : (a) A phase-contrast microscopy image of nematic structure in HUVECs.
(b) Half- integer topological defect in HUVECs.
Red : +1/2 topological defect , Blue : -1/2 topological defect

Acknowledgements
We thank K. Funamoto and M. Sano for valuable discussions.

References

1. Barrasa-Ramos, S., Blanch-Mercader, C. & Barakat, A. I. : “A nematic framework for sprouting angiogenesis” , bioRxiv 2025.11.12.688071 (2025).
2. Baeyens, N. et al. : “Vascular remodeling is governed by a VEGFR3-dependent fluid shear stress set point” , eLife 4, e04645 (2015).

Rectification of Active Brownian Particles in a 1D periodic ratchet

Kei Oriyose , Kota Mitsumoto , Shuji Ishihara

Graduate School of Arts and Sciences, Univ. of Tokyo

Given the same periodic potential landscape, passive and active particles respond in qualitatively different ways. Active articles can exhibit a finite steady drift once spatial symmetry is broken, whereas passive Brownian particles relax toward equilibrium with no steady current. Rectification in active particles under asymmetric environments is a prototypical nonequilibrium transport phenomenon in active matter (e.g., [1, 2]). However, a general framework that quantitatively predicts the sign and magnitude of the steady current for an arbitrary periodic ratchet potential is still lacking.

Here we analytically evaluate the steady-state current of ABPs in a one-dimensional periodic ratchet potential (Fig. 1(a)) and obtain a prediction applicable to an arbitrary potential profile. In the regime of small potential amplitude V_0, the rectified current scales as $J \propto V_0^3$, differently from usual current driven by external power supply. The theory quantitatively reproduces the rectified current observed in simulations (Fig. 1(b)). We also investigate the relation between rectification and entropy production rate in the resulting nonequilibrium steady state, and will report simulation results guided by the analytical prediction for J.

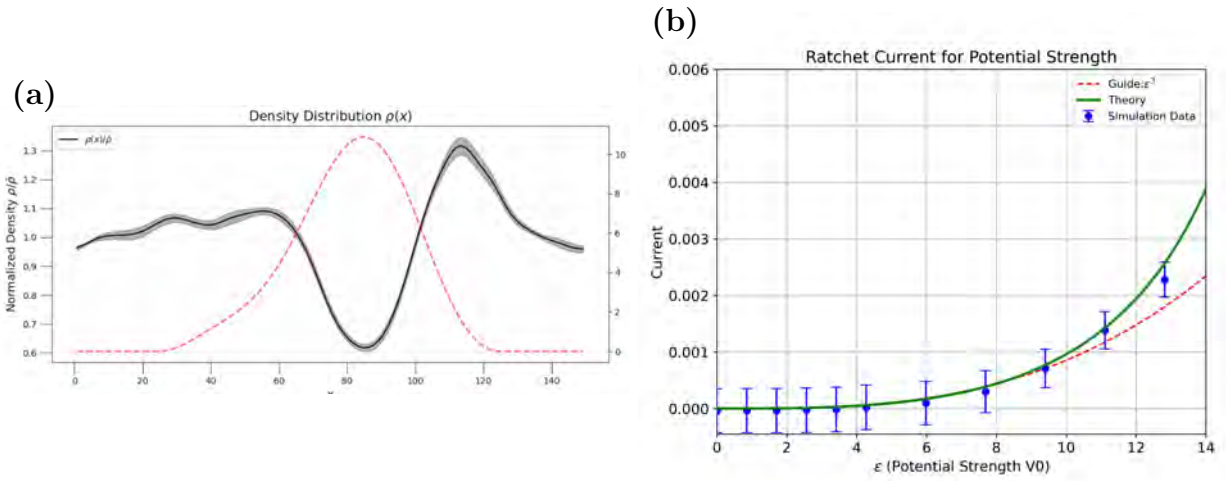

Figure 1: (a) Ratchet potential $V(x)$ used in simulations (red dashed line) and the corresponding steady-state density profile (black line). We use $V(x) = V_0 \cos^2(\pi x/W)\,[1 + \alpha \sin(2\pi x/W)]$, where α controls the left–right asymmetry. (b) Ratchet current J as a function of the potential amplitude V_0: theoretical prediction (solid line) and simulation results (blue dots with error bars). The scaling $J \propto V_0^3$ is indicated in the panel.

References

[1] C. J. Olson Reichhardt and C. Reichhardt, *Annu. Rev. Condens. Matter Phys.* **8**, 51–75 (2017).

[2] C. Roberts and Z. Zhen *Phys. Rev. E* **108**, 014139 (2023).

Just keep swimming: electrokinetic Janus particles under external fluid flow

Liliana Kershner[1], John Molina[2], Daiki Nishiguchi[1]
[1] Department of Physics, School of Science, Institute of Science Tokyo
[2] Department of Chemical Engineering, Graduate School of Engineering, Kyoto University

Rheotaxis is a well-documented navigation response to external fluid flow in biological systems.[1] Organisms exhibit orientation adjustment, upstream, and downstream swimming for biological advantage [1]. Increasingly, interest has been shown in reproducing these behaviors in synthetic, particulate systems, lending insight into the programmability of engineered swimmers through tuning of the flow field [2].

In our study we utilize electrokinetic Janus particles, which are instantaneously controlled via AC electric field, and exhibit a wide range of compelling behaviors such as translational motion, phase separation, polar-order flocking, and "active polymer" transport structures [3][4][5][6]. These particles lend themselves to rheotactic experiment due to the ease of tuning their motion through frequency and voltage parameters. Through applying a shear flow, we report our current experimental progress. We also present current efforts to numerically simulate this system with the smoothed-profile method [7].

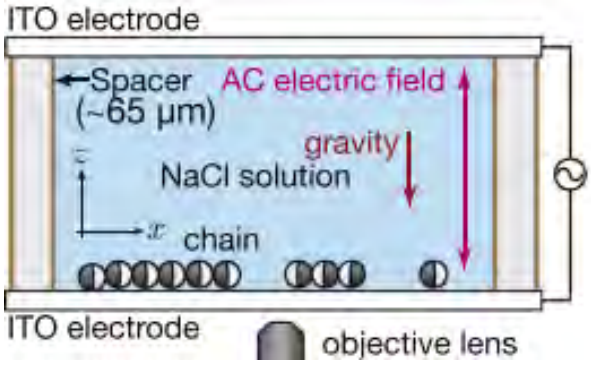

Static fluid setup of Janus experiment. Adapted from reference [5].

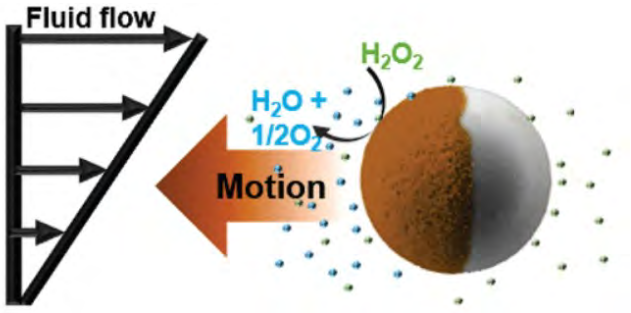

Rheotactic behavior of catalytic Janus particles [2].

[1] Uemura, N. A., *et. al*. "Rapid water flow triggers long-distance positive rheotaxis for thermophilic bacteria." The ISME Journal, 19(1). (2025).
[2] Sharan, *et al.* "Upstream rheotaxis of catalytic Janus particles". *ACS Nano*, 16, 3, 4599-4608. (2022)
[3] Das, *et. al*. "Flocking by Turning Away." Phys. Rev. X 14, 031008. (2024).
[4] Van der Linden, M. *et. al.* "Interrupted Motility Induced Phase Separation in Aligning Active Colloids." Phys. Rev. Lett. 123, 098001. (2019).
[5] Nishiguchi, D., *et al.* "Flagellar dynamics of chains of active Janus particles fueled by an AC electric field." New Journal of Physics, 20(1), 015002. (2018).
[6] Nishiguchi, D. "Deciphering Long-Range Order in Active Matter: Insights from Swimming Bacteria in Quasi-2D and Electrokinetic Janus Particles". Journal of the Physical Society of Japan, 92, 121007. (2023).
[7] Yamamato, *et. al*. "Smoothed profile method for direct numerical simulations of hydrodynamically interacting particles." *Soft Matter*,17, 4226-4253. (2021).

Jamming Transition of Chiral Active Particles

Duc T. Dam[1,*], Yuta Kuroda[2], Yoshihiko Nishikawa[1], Takeshi Kawasaki[3,4], Kunimasa Miyazaki[1]

[1]Department of Physics, Nagoya University, Nagoya 464-8602, Japan
[2]Institute for Theoretical Physics IV, University of Stuttgart, Heisenbergstrasse 3, 70569 Stuttgart, Germany
[3]D3 Center, The University of Osaka, Toyonaka, Osaka 560-0043, Japan
[4]Department of Physics, The University of Osaka, Toyonaka, Osaka, 560-0043, Japan
*Email: dam@r.phys.nagoya-u.ac.jp

Active matter is any system composed of self-propelling particles. All living things, from cells to animals, are active matter. The constant input of energy drives active matter systems out of equilibrium, leading to unique collective behavior such as bacterial swarms and bird flocks. At high densities, active matter systems undergo jamming transitions from fluid-like to disordered, solid-like states [1]. This transition is similar to that of passive particles, such as foams and colloids. Above the jamming transition, particles become confined by their neighbors, resulting in the dynamical arrest of the entire system. Among active matter systems, chiral active particles have recently drawn significant attention [2]. These particles exhibit asymmetric motion, breaking left-right symmetry as they follow circular trajectories due to chiral self-propelling forces. Previous studies on chiral active particles have primarily examined crystalline structures. Recent work has revealed that chiral active crystals with a finite orbital radius are more stable and non-chiral active crystals are less stable than equilibrium crystals [3]. However, it is unknown whether similar stabilization effects occur in disordered systems. The impact of chirality on disordered jammed states remains an open question, as the interaction between chiral motion and geometric constraints may result in different physical properties than those of crystalline systems.

In this study, we examine the effect of chirality on the stability of disordered jammed states using the chiral Active Brownian Particles (cABPs) model. Specifically, we study two-dimensional jammed particles driven by chiral self-propelling forces using numerical methods. By systematically tuning the chirality (orbital radius), activity (active velocity), and system size, we demonstrate two key findings. First, non-chiral jammed states (infinite orbital radius) are unstable – the critical active velocity required for melting vanishes in the thermodynamic limit, meaning any finite activity causes unjamming. Second, introducing chirality (finite orbital radius) dramatically stabilizes jammed states. This requires finite activity to induce melting, even in large systems. Increasing chirality further stabilizes the jammed phase. These results demonstrate that chirality stabilizes disordered active matter, which contrasts sharply with non-chiral systems, in which we believe jammed states exist only at zero activity and melt at any finite active velocity. Our findings shed new light on the fundamental physics of dense active matter and may help to explain the collective behavior observed in many biological systems.

References

[1] S. Henkes, F. Yaouen, and M. C. Marchetti, *Phys. Rev. E 84(4), 040301 (2011)*
[2] B. Liebchen and D. Levis, *Europhys. Lett. 139(6), 67001 (2022)*
[3] Y. Kuroda, T. Kawasaki, and K. Miyazaki, *Phys. Rev. Res. 7(1), L012048 (2025)*

Phase Diagram of Chiral Active Brownian Particles

Subhodeep Dey*[1], Yuta Kuroda[2], Yoshihiko Nishikawa[1], Takeshi Kawasaki[3], and Kunimasa Miyazaki†[1]

[1]Department of Physics, Nagoya University, Nagoya 464-8602, Japan
[2]Institute for Theoretical Physics IV, University of Stuttgart, Heisenbergstr. 3, 70569 Stuttgart, Germany
[3]D3 Center, Department of Physics, Osaka University, Toyonaka, Osaka 560-0043, Japan

Introduction: Self-propelling particles undergoing circular motion are known as chiral active matter. One of the simplest models of chiral active matter is the chiral Active Brownian Particles (cABP). The equation of motion of the cABP is given by,

$$\dot{\vec{r}}_i(t) = \gamma^{-1}\vec{f}_i(t) + v_0\vec{e}(\theta_i(t)); \qquad \dot{\theta}_i(t) = \Omega + \sqrt{\frac{2}{\tau_p}}\,\xi_i(t). \tag{1}$$

where r_i, f_i, θ_i, ξ_i are the position, interaction force, angular direction and Gaussian white noise of the i^{th} particle, respectively. Also, γ is the friction coefficient, v_0 is the velocity, Ω is the rotational frequency and τ_p is the persistent time fixed for all cABP particles. The chirality strength of the system can be defined using the radius of the circular motion of the particle trajectory, R=(v_0/Ω). Recently, Lei et al. [1] have studied cABP in the zero-noise ($\tau_p \to \infty$, in Eq.1) limit at low densities and shown that by increasing the density, a phase transition occurs from absorbing to a diffusive phase for various active chirality strengths, R. Kuroda et al. [2] have demonstrated that a phase transition occurs from diffusive (fluid) to solid phase in the high-density regime. In this work, we study the fate of the phase transition of the cABP system in the intermediate density regime (Fig.1).

Results and Discussion: In this work, we show the complete phase diagram of the chiral ABP in the zero noise ($\tau_p \to \infty$, in Eq.1) limit, where multiple phase transitions occur. We have used dynamical and structural order parameters to distinguish these phases clearly. First, we studied the dynamical behaviour using the diffusivity from the long-time dynamics of the mean-square displacement of the system. Then, for the structural properties, we have used the hexatic order parameter and the structure factor of the system. Using the dynamical properties of the system, we have shown that the reentrant transition for the chirality strength of around particle diameter takes place in the intermediate density of the system. This reentrant behaviour can be nicely verified using the hexatic order parameter as well as the structure factor of the system.

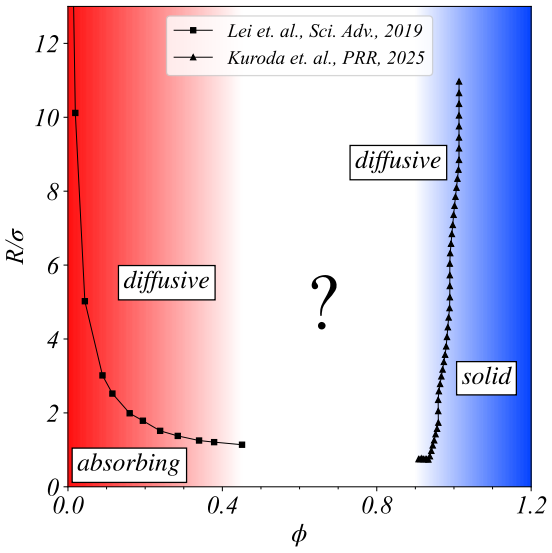

Figure 1: Phase diagram of the chiral Active Brownian Particles. Here, the known regions are low-density (red) absorbing and diffusive phase and high-density (blue) diffusive (fluid) and solid phase.

References:

1. Qun-Li Lei, Massimo Pica Ciamarra, and Ran Ni., "Nonequilibrium strongly hyperuniform fluids of circle active particles with large local density fluctuations", Sci. Adv.5, eaau7423 (2019).
2. Yuta Kuroda, Takeshi Kawasaki, and Kunimasa Miyazaki, "Long-range translational order and hyperuniformity in two-dimensional chiral active crystal", Phys. Rev. Research 7, L012048 (2025).

* subhodeep.dey@r.phys.nagoya-u.ac.jp
† miyazaki@r.phys.nagoya-u.ac.jp

Defect structure and dynamics in active nematic membranes

Yuki Hirota, Nariya Uchida

Department of Physics, Tohoku University, Sendai 980-8578, Japan

The interplay between the spatiotemporal dynamics of active matter and the geometry of deformable surfaces is an active area of research in biophysics and soft matter physics [1, 2]. In this study, we investigate the dynamics of active nematic liquid crystals on a nearly flat fluid membrane, focusing on the anisotropic coupling between the nematic director and the membrane curvature.

Our simulations reveal two distinct dynamic phases determined by the activity level. In the low-activity regime, we observe that topological defects are trapped by the local curvature of the membrane, resulting in a quasi-static configuration. As the activity increases, the system undergoes a transition where defects escape from these curvature traps and the membrane deformation cannot follow the rapid dynamics of the topological defects.

Furthermore, we examine the structure of the director field in this high-activity, nearly flat regime. Despite the suppression of macroscopic membrane deformation, we find a significant correlation between the local curvature and the "walls" (lines of high distortion arising from hydrodynamic instabilities [3]). Figure 1 shows the snapshot of the director field and the mean curvature.

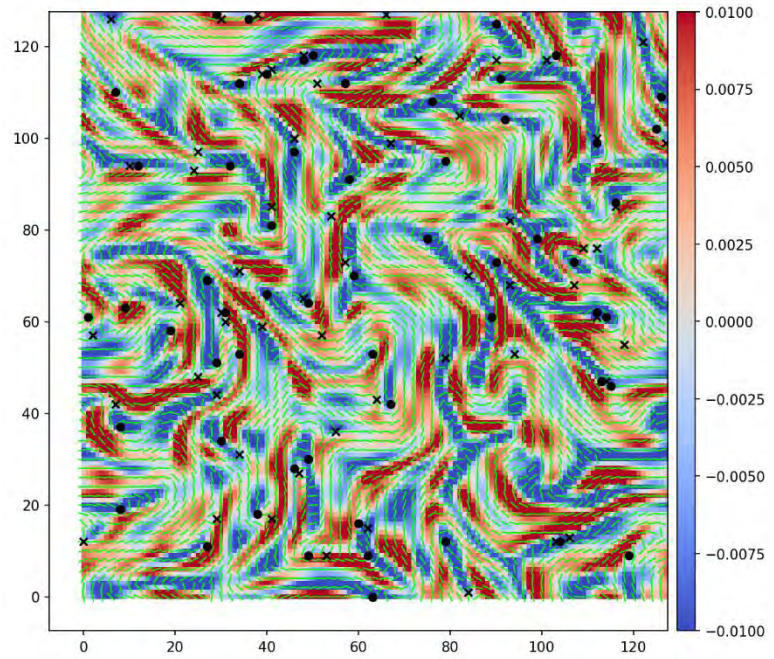

Fig. 1: Snapshot of the nematic director field (green lines) and the mean curvature field (red and blue), in the high-activity regime. A linear region of negative curvature flanked by positive curvature is observed, which coincides with the location of the wall in the director field. Black circles and crosses indicate +1/2 and -1/2 defects, respectively.

References

[1] Y. Maroudas-Sacks, *et al.*, Nat. Phys. **17**, 251 (2021).

[2] F. Vafa and L. Mahadevan, Phys. Rev. Lett. **129**, 098102 (2022).

[3] S. P. Thampi, *et al.*, EPL **105**, 18001 (2014).

Numerical simulation of active nematics in complex geometries with the Beris-Edwards model

Daisuke Miyokawa[1], **Hiroaki Ito**[2], **and Hiroyuki Kitahata**[2]

[1]Grad. Sch. of Sci. and Eng., Chiba Univ.,
[2]Grad. Sch. of Sci., Chiba Univ.

Active nematics, a class of active matter composed of polar or apolar units that exhibit orientational nematic order, have been extensively studied due to their characteristic phenomena, such as active turbulence and dynamics of topological defects [1]. It has been suggested that the geometry of the confining domain imposed on active nematic systems is closely related to the dynamics of topological defects, and that these defects are associated with apoptosis, indicating an intriguing connection to biological function [2].

In this study, we focused on the influence of domain shape on active nematics and investigated their behavior through numerical simulations. We performed simulations based on the Beris–Edwards model [3, 4] implemented in boundary-fitted coordinate (BFC), which enabled numerical calculations within complex geometries. We obtained orientational fields, velocity fields, and defect dynamics, which show that, in star-shaped domains, $+1/2$ topological defects are frequently induced in the regions near high boundary curvature. Based on these findings, we characterize the system behaviors and provide insights into the interplay between domain shape and the dynamics of topological defects.

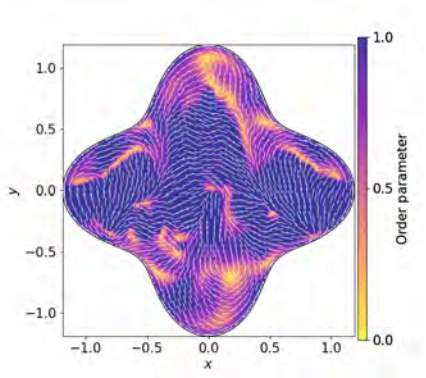

Fig.1: Alignment and order parameter field.

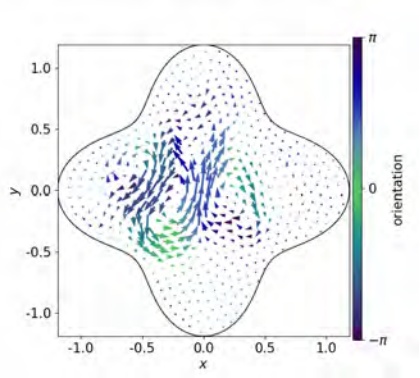

Fig.2: Velocity field corresponding to Fig.1.

References

[1] A. Doostmohammadi et al. Active nematics. *Nat. Commun.*, 9:3246, 2018.
[2] T. B. Saw et al. Topological defects in epithelia govern cell death and extrusion. *Nature*, 544:212–216, 2017.
[3] S. P. Thampi et al. Instabilities and topological defects in active nematics. *Europhys. Lett.*, 105:18001, 2014.
[4] R. Saghatchi et al. Development of smoothed particle hydrodynamics method for modeling active nematics. *Int. J. Numer. Methods Eng.*, 124:159–182, 2023.

Mechanical model of cell crawling with torque-free rotation

Daisuke Katayama, **Mitsusuke Tarama**

Department of Physics, Kyushu University

Dynamics of cells crawling on a substrate has been studied from various perspectives. In recent years, chirality of cells has been receiving increasing attention. In experiments, some species of cells show the trajectories statistically curved to the right or left [1]. Although there are many theoretical studies on cell migration, less have been conducted on such a rotational motion.

In this research, we develop a mechanical model for cell crawling with torque-free rotation, in which a single cell is represented by two particles connected by a viscoelastic spring. Previous research, which omits the rotational motion, demonstrated that the periodic changes in the natural length of the viscoelastic spring and the time-dependent substrate adhesion enable the model cell to migrate spatially under force-free conditions [2]. To include the active rotational motion of cells, we modified the model by introducing a torque dipole. By this extension, we achieved rotational motion of the cell under torque-free condition where no net torque exists.

This model can be separated mathematically into translational and rotational parts. When focusing on rotational motion, the dynamics of cell can be classified into four types. Each type could be characterized by three quantities: the rotation angle around the center of mass (COM), the migration length along the COM trajectory, and the net displacement of the COM. Furthermore, by combining this result with translational motion, we can reproduce similar dynamics that are observed for actual cells.

References

1. Atsushi Tamada and Michihiro Igarashi, “Revealing chiral cell motility by 3D Riesz transform-differential interference contrast microscopy and computational kinematic analysis”, *Nat. Commun*. **8**, 2194(2017)
2. Mitsusuke Tarama and Ryouichi Yamamoto, “Mechanics of Cell Crawling by Means of Force-free Cyclic Motion”, *J. Phys. Soc. Jpn.* **87**, 044803(2018)

Self-aligned tension gradient induces antiparallel circulation pattern in confluent cell monolayers

Ryunosuke Karimata[1], **Shuhei A. Horiguchi**[2], **and Satoru Okuda**[2,3]

[1]Division of Nano Life Science, Graduate School of Frontier Science Initiative, Kanazawa University
[2]Nano Life Science Institute, Kanazawa University
[3]Sapiens Life Sciences, Evolution and Medicine Research Center, Kanazawa University

The emergence of dynamic order and patterns is a central paradigm in active matter systems and plays a crucial role in the dynamic processes of biological systems. Particularly, multicellular systems can exhibit diverse spatiotemporal patterns due to the multifunctionality of the cells. For example, self-propelled force at the cell-substrate interface leads to flocking and rigid-body rotation in the confluent epithelial cells. On the other hand, cells can also move by exchanging anisotropic forces with surrounding adjacent cells. Indeed, collective cell migration within 3D tissues or complex collective movements during early development are driven by polarized active tensions at cell-cell interface. However, the dynamic order and pattern formation of multiple cells moving via such active forces satisfying force balance have not been sufficiently explored.

In this study, we perform numerical simulations using a two-dimensional (2D) vertex model to explore the collective cell behaviors that can arise from polarized, force-balanced interactions. 2D vertex model represents a confluent cell monolayer as a polygonal tiling, where each polygon corresponds to a cell. We consider the mixture of nonmotile cells and polar motile cells which can migrate by tension gradient at the cell-cell interface along with its own polarity. The polarity of each cell is given the ability to align in the orientation of the cell's own velocity, called self-alignment, and to rotationally fluctuate. Starting from the randomly mixed configurations, we predict the behavior of the systems varying the alignment rate and the rotational noise intensity of the self-alignment.

As a result, we found that the phase separation occurs when alignment rate is high: motile cells spontaneously cohered and formed domains surrounded by nonmotile cells. Remarkably, within each domain, motile cells align to form a closed-loop circulation, with neighboring circulations oriented in antiparallel directions. This finding indicates that such antiparallel cell circulation patterns emerge from self-aligned tension gradient. To clarify the elementary processes underlying cell circulation, we examined the pairwise movement of motile cells. We found that persistent translational motion is frequently observed and that the interfacial tension between motile cells vanishes, indicating that once a head-to-tail configuration forms, the pair behaves as a mechanically self-stabilizing unit. Finally, we constructed a simple mathematical model describing the motion of circulations and uncovered that the antiparallel patterns are stabilized by self-aligned active forces that satisfy the force balance. Taken together, these findings show that self-aligned tension gradients constitute a robust and previously overlooked mechanism for producing dynamic microscopic patterns in multicellular systems.

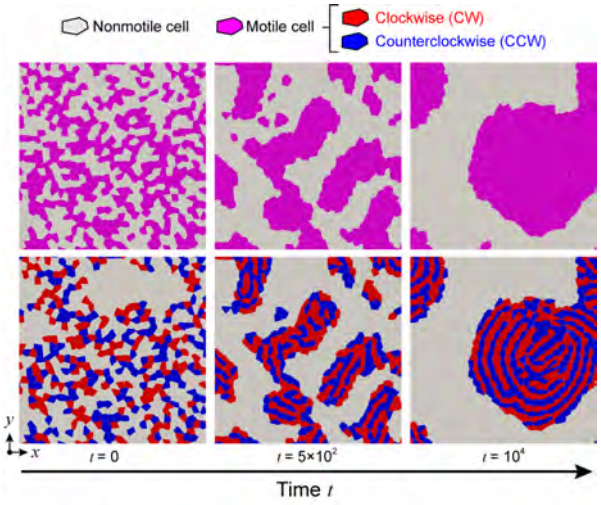

Figure 1. Phase separation and antiparallel circulation pattern within a motile cell domain.

Acknowledgements
We are very grateful to Dr. T. Hiraiwa at the Institute of Physics, Academia Sinica, and S. Sawai at the Graduate School of Arts and Science, University of Tokyo useful discussions. We thank our lab members for the time they spent in English proofreading, practicing, and so forth. This work was supported by WISE Program for Nano-Precision Medicine, Science, and Technology of Kanazawa University by MEXT.

Euglena's Phototaxis and Bioconvection under Multiple Light Sources

Naoyasu Morino[1], **Nobuhiko J. Suematsu**[2]

[1]Graduate School Advanced Mathematical Sciences, Meiji University
[2]Meiji Institute for Advanced Study of Mathematical Sciences (MIMS), Meiji University

Euglena is a photosensitive microorganism and exhibits positive phototaxis by swimming toward weaker light and negative phototaxis by moving away from stronger light. When strong light is directed from below onto a culture of *Euglena*, they ascend to the upper layer due to negative phototaxis. However, this state is unstable due to the weight of Euglena, and some *Euglena* will descend because of gravity. The descending *Euglena* encounter strong light from below again, prompting negative phototaxis to drive them toward the interface again. These actions repeat, leading to the formation of bioconvection through the interaction of negative phototaxis and gravity. The points where *Euglena* descend due to gravity appear as spots when viewed from above. This phenomenon occurs in multiple locations, resulting in the formation of a set of points (Fig.1).

Most studies on bioconvection of *Euglena* have concentrated on cases where light is only irradiated from below. In contrast, we investigated how the bioconvection pattern of *Euglena* changes when light is illuminated from both above and below.

In this study, we conducted two types of experiments: bioconvection experiments and single-cell (individual-level) analyses. In both experiments, we fixed a strong light source on one side and varied the light intensity from the opposite side, which allowed us to clarify the correspondence between bioconvection patterns and individual motile responses. In particular, we focused on the spot structures formed by bioconvection and evaluated the number of spots, their temporal evolution, and the spacing between spots using Voronoi analysis.

Our analysis revealed that when weak light is irradiated from above, the resulting spot patterns are unique, suggesting a significant influence from *Euglena*'s positive phototaxis. Additionally, we employed a mathematical model using the Rayleigh number—a dimensionless quantity representing the ease of bioconvection occurrence—to clarify the mechanisms underlying this phenomenon.

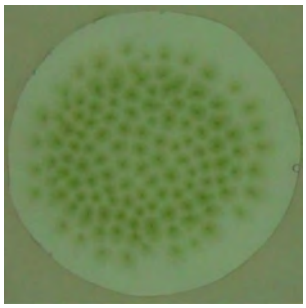

Fig.1: Bioconvection of Euglena

References

1. Erika Shoji, Shunsuke Izumi, Hikaru Nishimori, Akinori Awazu, Makoto Iima (Graduate School of Science, Hiroshima University),
   "ミドリムシ生物対流の局在構造と走光性" (2014), vol.1900: 76-84
2. Nobuhiko J. Suematsu (Graduate School of Advanced Mathematical Sciences, Meiji University),
   "微生物の走光性にともなう局在対流パターンの光応答性" (2014), vol.1900: 85-90

Motility analysis of the density wave propagation in Ciliate *Tetrahymena* suspension

Ryuhei Itoh[A], Kohei Okuyama[1], Ibuki Kawamata[1], Marie Tani[1], Akira Kakugo[1], Masatoshi Ichikawa[1,2]

Dept. of Phys. Kyoto Univ.[1], Grad. Sch. Integ. Sci. Life, Hiroshima Univ.[2]

In nature, birds, fish, and mammals form school, flocks, and herd exhibiting autonomous order and collective behavior. These organized structures emerging from such biological collectives are intensively studied in the field of active matter [1]. As one of the interesting phenomena, some biological systems have been reported to exhibit ordered and spatiotemporal patterns such as propagating density waves and alignments of traveling direction. For example, in bacterial systems, individual chemotactic responses combined with the diffusion of nutrients give rise to reaction diffusion density waves [2], whereas in the Vicsek model, alignment interactions among self-propelled particles are known to generate propagating waves [3]. Understanding these waves mechanisms underlying these collective waves is a key challenge in unravelling the principles of collective motion.

In this study, we focus on pattern formation in dense suspensions of the swimming microorganism *Tetrahymena*. While previous studies have reported steady-state phenomena such as bioconvection [4] and mesoscale turbulence in these cell suspensions, propagating wave-like collective dynamics have not been observed. To tackle the issue, we designed a quasi-two-dimensional system by limiting the fluid depth to suppress the steady-state fluid phenomena and successfully captured the formation and propagation of collective density waves (Fig 1).

To enhance how these waves emerge and propagate spatially, we employed Particle Tracking Velocimetry (PIV) to analyze the time evolution of cell motility and spatial distribution. In this conference, we will detail the experimental findings and discuss the mechanisms underlying this newly observed collective wave phenomenon in *Tetrahymena* suspensions.

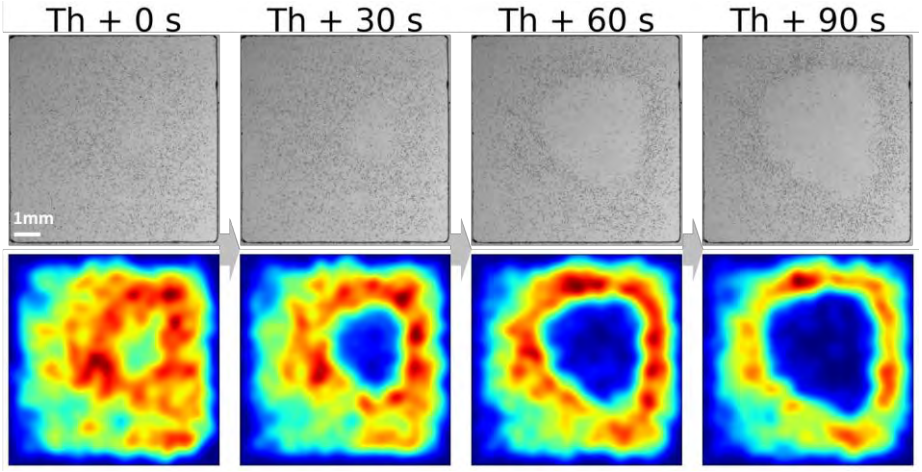

Fig 1. Temporal evolution of density waves
(Top: Original images. Bottom: Density map.)

References
[1] D. J. T. Sumpter, *Phil. Trans. R. Soc.* B 361, 5-22(2006).
[2] J. Adler, *J. Supramol. Struct.* **4**(3), 305–317 (1976).
[3] W. Ngamsaad, & S. Suantai. *Physical Review E*, **98**, 062618 (2018).
[4] A. Kage et al., *Zoological Science*, 28, 206-214 (2011).

Cellular-Scale Mechanism of Optimal Substrate Stiffness for Cell Crawling

S. Nakamura, **M. Tarama**

Dept. of Phys. Kyushu Univ.

Cell migration plays an important role in morphogenesis and wound healing, and cells respond to environments by altering their migratory behavior. In particular, the phenomenon in which cells sense substrate stiffness and adjust their migratory behavior is known as Durotaxis [1]. It is known that cells modulate their adhesion strength to the substrate depending on substrate stiffness, and it is believed that such changes in subcellular-scale adhesion influence cellular scale deformation and adhesion dynamics, thereby affecting cell migration. However, direct evidence for this scenario has been limited.

In our study, we introduced cell-migration model that change substrate-adhesion characteristics at subcellular scale and investigated the resulting mechanisms at the cellular scale. We analyzed cell migration on substrates with uniform stiffness. Interestingly, as the substrate stiffness increased, the cell migration speed increased up to a certain stiffness but then began to decrease beyond this optimal stiffness (Fig1). This non-monotonic trend has also been reported in experimental studies, and our results are consistent with those observations [2]. We investigated the mechanism underlying the existence of optimal substrate stiffness by focusing on cell deformation and substrate adhesion at the cellular scale (Fig2). As the substrate stiffness increased, cell deformation was suppressed, whereas the asymmetry of adhesion between the front and back of the cell was enhanced. Furthermore, we derived an equation that relates cell migration speed to deformation and adhesion asymmetry, and found that the cell migration speed is maximized at a substrate stiffness where the cell undergoes substantial deformation and exhibits a sufficiently large asymmetry in adhesion.

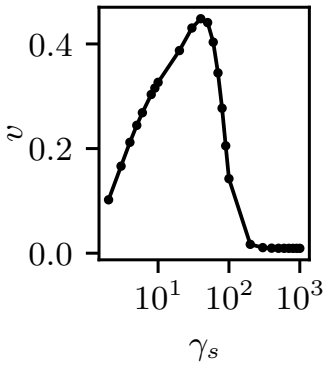

Figure 1: Dependence of cell migration speed on substrate stiffness.

Substrate stiffness γ_s	Adhesion asymmetry Z_{diff}	Cell deformation Q	Migration speed v	Two-element sketch
Too soft	✗	✓	✗	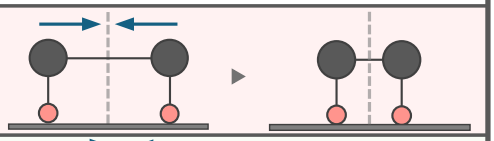
Optimal stiffness	✓	✓	✓	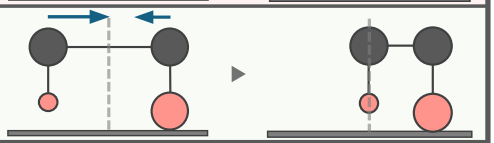
Too stiff	✓	✗	✗	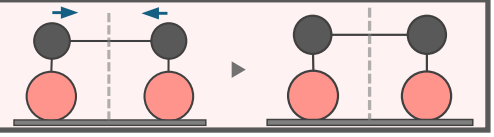

Figure 2: Schematic illustration of the intuitive mechanism underlying the existence of an optimal substrate stiffness.

References
1. Lo et al., *Biophys. J.* **79**, 144-152. (2000).
2. Sean et al., *Nature*. **385**, 537-540. (1997).

Collective Dynamics of Highly Packed Elliptical Cells

Nen Saito[1], Kohei Okuyama[2], Seiya Takamura[3], Kiwamu Yoshii[4], Masatoshi Ichikawa[3]

1. Life Science Center for Survival Dynamics, University of Tsukuba
2. Department of Physics, Kyoto University, Kyoto 606-8502, Japan
3. Graduate School of Integrated Sciences for Life, Hiroshima University
4. Department of Applied Physics, Tokyo University of Science

Several types of two-dimensional collective dynamics in microorganisms have been reported so far. In this study, we performed simulations of elliptically shaped self-propelled particles to recapitulate the experimentally observed collective behaviors of *Tetrahymena*. Following Ref. 1, we developed a mathematical model of elliptical self-propelled particles under densely packed conditions.

Both the experimental data and simulation results show the coexistence of turbulence-like and glass-like behaviors. A representative simulation snapshot in the high-density regime is presented in Fig. 1a. Most cells exhibit only small displacements (white cells), whereas a fraction of cells display large displacements with coherent migration directions (colored cells), indicating the presence of dynamical heterogeneity. In addition, particle trajectories contain multiple vortices (inset of Fig. 1a). Analysis of the velocity correlation and the corresponding correlation length reveals hallmarks of critical behavior (Fig. 1b, c).

We will also discuss possible implications of these phenomena.

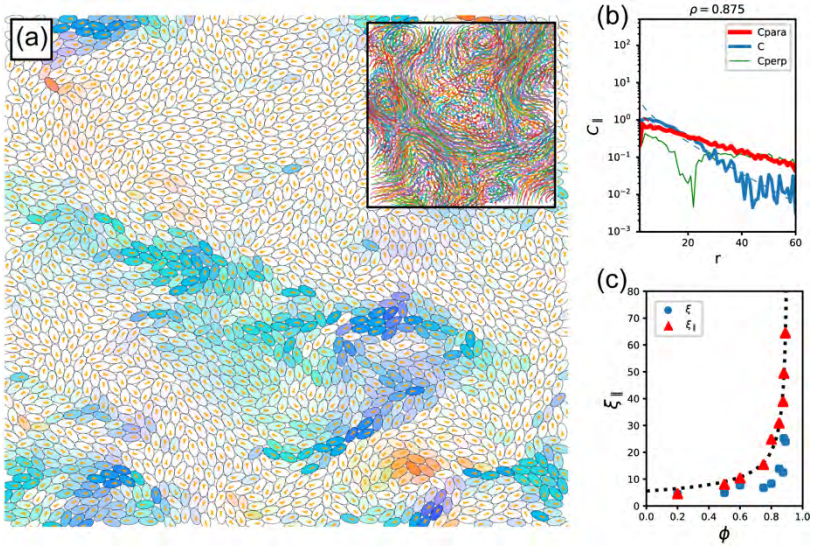

Fig1: (a) A simulation snapshot with 2000 cells. Color code represents displacement and its direction. Inset represents trajectories. (b) Velocity correlation function for volume fraction 0.875. (c) Density dependence of the correlation length.

Ref1. N. Saito, S. Ishihara, *Science Advances* 10 (19), eadi8433 (2024)

Synchronous beating of cardiac cells by elastic interactions

Akinari Tomiie, Nariya Uchida
Department of Physics, Graduate School of Science, Tohoku University

The pumping function of the heart is maintained by the synchronous beating of numerous cardiomyocytes. Recent experiments suggest that sarcomeres, the contractile units of cardiomyocytes, synchronize not only through biochemical signals but also via elastic mechanical interactions [1]. Previous studies have examined the stability of in-phase and anti-phase synchronization with respect to cell orientation using static elastic energy analyses that model cardiomyocytes as force dipoles [2].

In the present study, we extend this approach and develop a mathematical model to describe the dynamics of mechanically driven synchronization. The actomyosin contractile mechanism of the sarcomere is well described by the following nonlinear equation:

$$\ddot{x_i} - \varepsilon\left(1 - \dot{x_i}^2\right)\dot{x_i} + x_i = f_{\mathrm{int}} \tag{1}$$

Here, x_i denotes the displacement of the cardiac cell i from its natural length. The second term represents energy injection via ATP hydrolysis at low velocities and dissipation at high velocities. The force f_{int} arises from the interaction with other cells. Equation (1) with $f_{\mathrm{int}} = 0$ is known as the Rayleigh equation and exhibits a limit cycle.

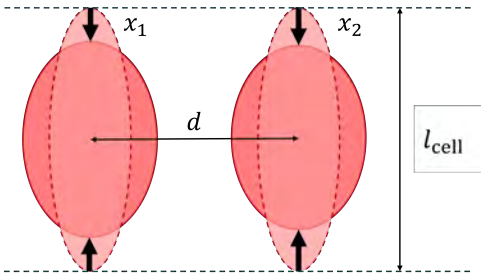

Fig.1: Schematic picture of two cardiomyocytes arranged side-by-side, with the natural cell length l_{cell}, intercellular distance d, and displacements x_1, x_2.

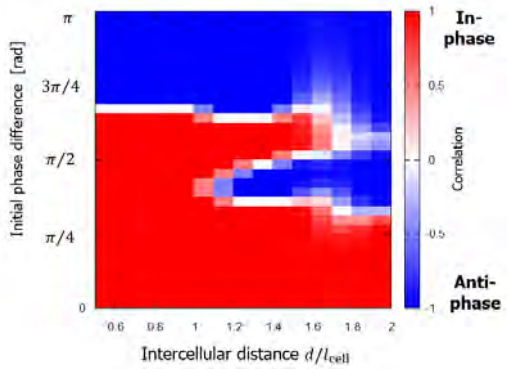

Fig.2: Dependence of the final synchronized states (red: in-phase, blue: anti-phase) on the initial phase difference and intercellular distance.

We consider a system of two cardiomyocytes placed on a semi-infinite elastic substrate with various relative orientations. Contraction of the cells induces deformation of the elastic medium, resulting in mechanical interaction. For the configuration shown in Fig.1, we find numerically that either the in-phase or anti-phase synchronization is achieved depending on the initial phase difference and the intercellular distance, as shown in the state diagram (Fig.2). The bistability suggests the importance of dynamical modeling of synchronous beating beyond energy minimization principle.

References

[1] I. Nitsan *et al.*, *Nat. Phys.* **12**, 472–478 (2016).
[2] O. Cohen and S. A. Safran, *Soft Matter* **12**, 6088–6095 (2016).

Phototaxis of the Self-propelled Droplet -- Stochastic Response to the Light Intensity Gradient

Keigo Takeda[1], **Nobuhiko J. Suematsu**[1,2]

[1]Graduate School of Advanced Mathematical Sciences, Meiji University
[2]Meiji Institute for Advanced Study of Mathematical Sciences (MIMS), Meiji University

The Belousov-Zhabotinsky (BZ) reaction is a typical chemical oscillatory reaction that bifurcates into a steady state and an oscillatory state depending on physicochemical conditions. Ruthenium, as a metal catalyst for the BZ reaction, is known to be used for realizing photosensitivity. It is known that when exposed to strong light, it approaches a reduced steady state.

Furthermore, it is known that the BZ droplet prepared in an oil containing the surfactant monoolein (MO) exhibits self-propelled motion [2]. This self-propelled motion depends on the chemical condition inside the droplet. It has been reported that photosensitive BZ droplets with a ruthenium catalyst can control the mode of droplet motion in response to the light intensity [1].

In this study, self-propelled BZ droplets containing ruthenium were prepared under a light-intensity gradient. The results showed that photosensitive BZ droplets moved toward the dark side, namely, negative phototaxis. In order to uncover the underlying mechanism of the negative phototaxis, we measured the movement direction of the droplets. As a result, the movement direction was almost isotropic in a short time. Therefore, we consider that the negative phototaxis realized by stochastic process as is observed in bacterial chemotaxis [3].

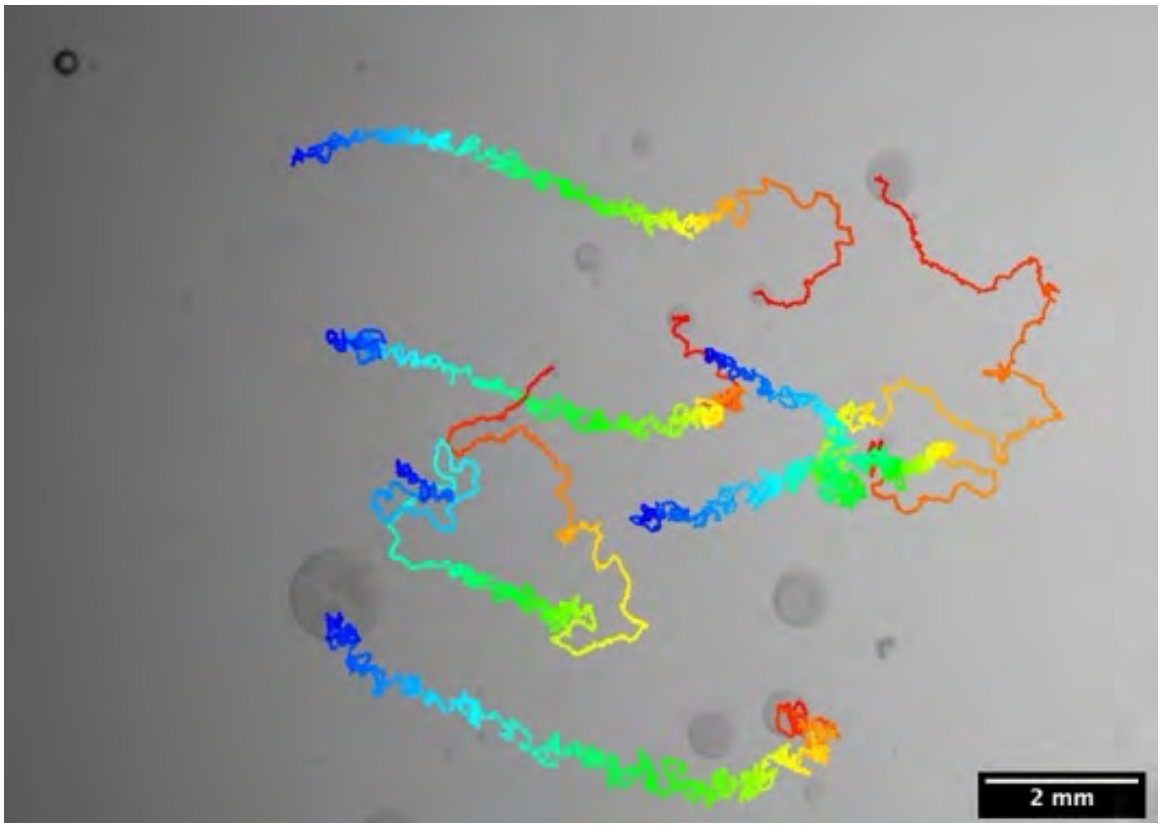

Fig.1: Trajectory of droplet motion. (Time is passing from red to blue.)

References

1. Nobuhiko J. Suematsu and Satoshi Udagawa:” Real-time Mode-switching of a Self-propelled Droplet Controlled by the Photosensitive Belousov–Zhabotinsky Reaction” (2023)
2. Nobuhiko J. Suematsu:”Oscillation of Speed of a Self-Propelled Belousov–Zhabotinsky Droplet” (2016)
3. Yuko Hamano, Kota Ikeda, Kenta Odagiri, Nobuhiko J. Suematsu:” Reproduction of bacterial chemotaxis by a non-living self-propelled object” (2023)

Light-written reconfigurable active matter with memory: optically creating, coupling, and erasing self-propelled droplets

Shinya Hakuta, **Masayuki Naya, Mamoru Sato, Jintaro Shiina, Toshiharu Saiki**

Graduate School of Science and Technology, Keio University

Droplet-based active matter systems have attracted significant attention due to their soft interfaces and relevance to biological cells and soft robotics. However, many existing systems rely on pre-existing droplets and therefore lack intrinsic reconfigurability, such as the ability to nucleate or erase active units on demand.

We discovered that when a mixed solution of polyethylene glycol (PEG) and ethanol is confined in a micro-gap between glass plates, weak laser irradiation (~1 mW) into a vapor bubble region induces the formation of a flattened microdroplet that follows the laser position. This droplet generation arises from a solutal Marangoni effect driven by laser-induced concentration gradients, forming a nonequilibrium steady state in which the droplet stably exists. Moreover, by turning the laser on and off or repositioning it, droplets can be reversibly written and erased in situ, enabling on-demand creation and removal of active particles.

Remarkably, the droplet spontaneously begins to rotate around the laser spot and continues for tens of minutes with a well-defined frequency on the order of a few hertz. Despite the axisymmetric configuration of both the liquid and the laser field, the system exhibits spontaneous symmetry breaking that stabilizes the rotation. The droplet leaves behind a PEG-rich trail with higher surface tension, which acts as a time-delayed feedback and enhances the tendency of the droplet to revisit its own previous paths. This memory effect introduces non-reciprocity into the dynamics and stabilizes the persistent rotation.

In this presentation, we will discuss the generation, control, and self-organized motion of the droplets, as well as interactions among multiple droplets, supported by numerical simulations that elucidate the underlying mechanisms.

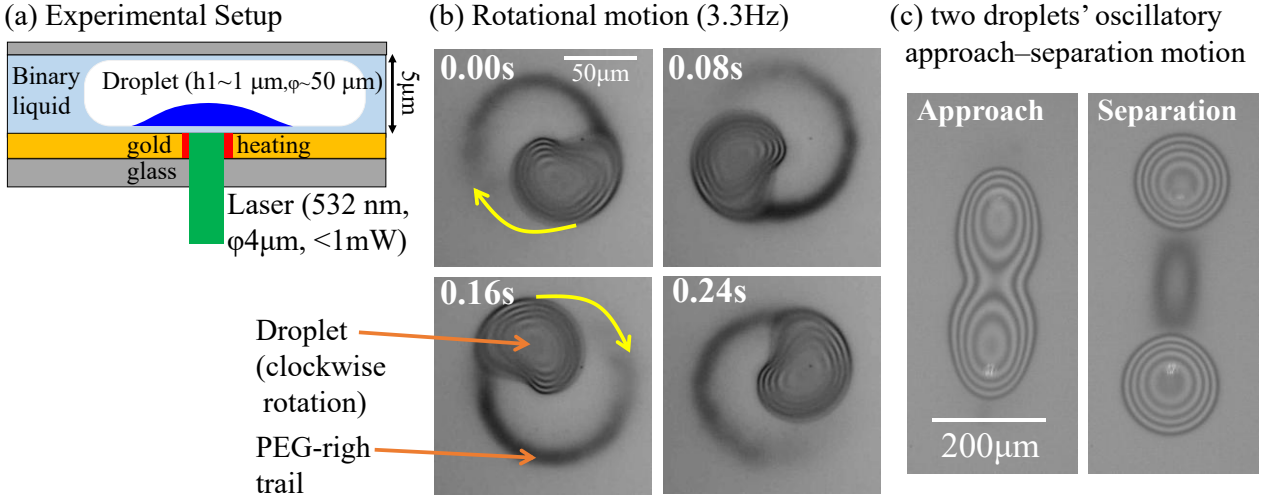

Figure. Light-written self-propelled droplets. (Left) Schematic of laser-induced droplet generation in a PEG/ethanol micro-gap. (Center) Spontaneous rotational motion leaving a PEG-rich trail. (Right) Oscillatory approach–separation dynamics between two droplets.

References

1. Shinya Hakuta *et. al.*, "Real-Time Visualization of Solutal Marangoni Convection in Sub-100 nm Precursor Films Using Laser-Generated Droplet Probes", *Langmuir* **41**, 31927–31935 (2025).
2. Shinya Hakuta *et. al.*, "Laser-induced microdroplets", *Proc. SPIE* 13703, Optical Manipulation and Structured Materials Conference 2025, 1370306 (2025).
3. Yuka Takamatsu *et. al.*, "All-Optical Rapid Formation, Transport, and Sustenance of a Sessile Droplet in a Two-Dimensional Slit with Few-Micrometer Separation", *Micromachines* **14**, 1460 (2023).

Coalescing dynamics of self-propelled droplets on substrates

Yuki Koyano[1], **Nariya Uchida**[2]

[1]Graduate School of Human Development and Environment, Kobe University
[2]Graduate School of Science, Tohoku University

Droplets that actively modify the surrounding interfacial tension can self-propel on a substrate [1]. They exhibit a variety of dynamical behaviors, including chasing, splitting, and coalescence [2]. In this study, we investigate the coalescence process of such droplets based on a model of a liquid film thickness profile derived from the Navier-Stokes equations with the lubrication approximation [3,4].

Under partial wetting conditions, a liquid film with uniform thickness becomes unstable and breaks up into droplets. After the breakup, the droplets begin to self-propel in random directions and repeatedly coalesce through collisions. We first discuss the droplet size that emerges at the onset of film instability by linear stability analysis. We also investigate the dynamics of the number of droplets as it changes through repeated coalescence events.

Acknowledgements
This work was supported by the JSPS Core-to-Core Program "Advanced core-to-core network for the physics of self-organizing active matter (JPJSCCA20230002)," JSPS KAKENHI Grants No. JP24K16981, and also the Cooperative Research Program of "Network Joint Research Center for Materials and Devices" (No. 20251011).

References

1. Yutaka Sumino, Nobuyuki Magome, Tsutomu Hamada, and Kenichi Yoshikawa: "Self-Running Droplet: Emergence of Regular Motion from Nonequilibrium Noise", *Phys. Rev. Lett.* **94**, 068301/1-4 (2005).
2. N. J. Cira, A. Benusiglio & M. Prakash: "Vapour-mediated sensing and motility in two-component droplets", *Nature* **519**, 446-450 (2015).
3. S. M. Troian, E. Herbolzheimer, and S. A. Safran: "Model for the Fingering Instability of Spreading Surfactant Drops", *Phys. Rev. Lett.* **65**, 333-3366 (1990).
4. Uwe Thiele, Karin John, and Markus Bär: "Dynamical Model for Chemically Driven Running Droplets", *Phys. Rev. Lett.* **93**, 027802/1-4 (2004).

Topological Defects in Spiral Wave Chimera States

Lintao Liu*, Nariya Uchida

[1] *Department of Physics, Tohoku University, Sendai 980-8578, Japan*

*liu.lintao.s2@dc.tohoku.ac.jp

Chimera states—characterized by the coexistence of coherent and incoherent domains—pose a fundamental challenge in the study of self-organization. While the spatial patterns in chimera states are extensively documented, a quantitative framework for their topological properties is still lacking. Here we investigate the dynamics of spiral wave chimeras in the non-local Sakaguchi-Kuramoto model with a top-hat coupling on a two-dimensional square lattice. Using winding number analysis, we characterize the topological properties of the incoherent spiral cores varying the phase lag α. Figure 1(a) shows the distribution of ± 1 defects in an incoherent core. We use the total positive winding number n_+ (the number of $+1$ defects) as the central tool for our topological analysis.

Our results identify two distinct dynamical regimes: (1) Linear Geometric Scaling: A perturbative self-consistent-field analysis for $\alpha \ll 1$ shows that the incoherent core radius scales linearly with α, in agreement with the previous results for Gaussian coupling [1]. (2) Exponential Topological Growth [Fig.1(b)]: Within the stable chimera regime, the average total positive winding number $\overline{n_+}$ follows an exponential growth law, $\overline{n_+} = ae^{b\alpha}$, signaling a transition from simple core expansion to active topological excitation. Furthermore, in the distribution of n_+, we identify a critical threshold α^* marking a transition from binomial-like to Poisson-like behavior, accompanied by an abrupt increase in the Shannon entropy [Fig.1(c)]. This transition suggests a shift from a constrained state to an unconstrained state of topological defects, drawing a physical analogy to the Berezinskii-Kosterlitz-Thouless (BKT) binding-unbinding transition.

Our findings propose the winding number n_+ as a robust metric for quantifying the complexity of chimera states and offer new insights into the statistical order underlying topological defects in non-equilibrium systems.

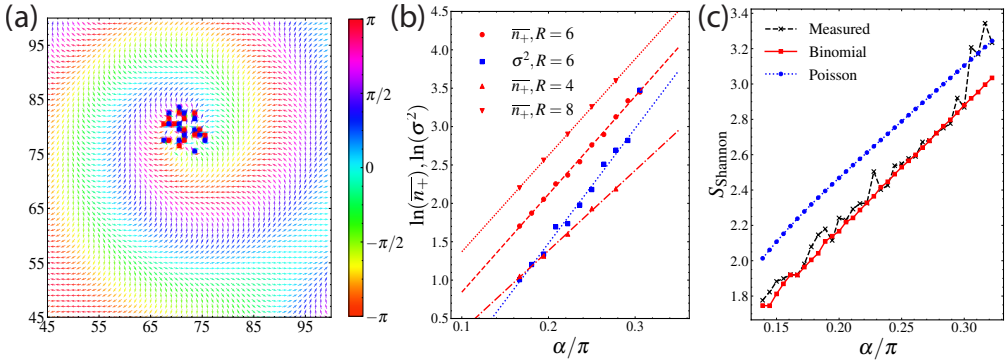

Figure 1: (a) Snapshot of spiral wave chimeara states for the phase lag $\alpha = \pi/4$ and coupling range $R = 6$. The colorscale shows the phase, and ± 1 defects are shown by red and blue squares (resp.) (b) Dependence of the average $\overline{n_+}$ and variance σ^2 of the total positive winding number on the phase lag α. (c) Comparison of the measured Shannon entropy with the theoretical binomial and Poisson entropy. (Adapted from Ref.[2].)

References

[1] E. A. Martens, C. R. Laing, and S. H. Strogatz, *Phys. Rev. Lett.* **104**, 044101 (2010).

[2] L. Liu, N. Uchida, arXiv: 2511.21058 (2025).

Global bifurcation analysis of nonreciprocal pattern transitions near O(2)-symmetric Takens-Bogdanov point

Yuta Tateyama[1], Daniel Greve[2], Hiroaki Ito[1], Shigeyuki Komura[3], Hiroyuki Kitahata[1], Uwe Thiele[2]

[1]Department of Physics, Graduate School of Science, Chiba University, Japan
[2]Institute of Theoretical Physics, University of Münster, Germany
[3]Wenzhou Institute, University of Chinese Academy of Sciences, China

Nonreciprocity, characterized by the breakdown of Newton's third law, has emerged as a key concept driving intricate spatiotemporal dynamics in active matter [1, 2, 3]. While the transition from static patterns to traveling waves is a signature of nonreciprocal pattern formation, the precise transition routes and the underlying bifurcation structures remain to be fully elucidated. In this study, we investigate the onset of pattern dynamics by focusing on a specific codimension-two singularity. While often termed an exceptional point in non-Hermitian physics [4], this point is identified as an O(2)-symmetric Takens-Bogdanov (TB) bifurcation within the framework of bifurcation theory [5].

We employ the nonreciprocal Swift-Hohenberg (NRSH) model [1, 6, 7] as a representative system. The NRSH model is characterized by a finite characteristic wavenumber and exhibits nonreciprocal phase transitions:

$$\partial_t \phi = \left[\varepsilon + \delta - (1+\partial_x^2)^2\right]\phi - \phi^3 - (\chi+\alpha)\psi,$$
$$\partial_t \psi = \left[\varepsilon - \delta - (1+\partial_x^2)^2\right]\psi - \psi^3 - (\chi-\alpha)\phi.$$

We derive a reduced system of coupled amplitude equations via spatial Fourier one-mode reduction [7]. Subsequently, using near-identity transformations, we reduce the NRSH model around the O(2)-symmetric TB bifurcation point to its normal form. This derivation establishes an explicit mapping between the physical parameters and the unfolding parameters of the normal form, facilitating a unified understanding of the global bifurcation structure. Crucially, we demonstrate that while the generic O(2)-symmetric TB bifurcation theoretically admits 29 distinct scenarios [5], the restriction to local interactions rigidly limits the system to only two possible scenarios. We will present comprehensive bifurcation diagrams and phase diagrams to elucidate the routes to traveling waves organized by this codimension-two bifurcation point.

[1] M. Fruchart, R. Hanai, P. B. Littlewood, V. Vitelli, *Nature* **592**, 363–369 (2021).
[2] S. Saha, J. Agudo-Canalejo, R. Golestanian, *Phys. Rev. X* **10**, 041009 (2020).
[3] T. Frohoff-Hülsmann, U. Thiele, *Phys. Rev. Lett.* **131**, 107201 (2023).
[4] W. D. Heiss, *J. Phys. A: Math. Theor.* **45**, 444016 (2012).
[5] G. Dangelmayr, E. Knobloch, *Philos. Trans. R. Soc. Lond. A* **322**, 243–279 (1987).
[6] D. Schüler, S. Alonso, A. Torcini, M. Bär, *Chaos* **24**, 043142 (2014).
[7] Y. Tateyama, H. Ito, S. Komura, H. Kitahata, *Phys. Rev. E* **110**, 054209 (2024).

Pattern selection mechanism depending on initial conditions in immiscible two-layer thermal convection

Mizuki Nakamura[1], **Hiroaki Ito**[2] , **Hiroyuki Kitahata**[2]

[1]Graduate School of Science and Engineering, Chiba University, Chiba, Japan
[2]Graduate School of Science, Chiba University, Chiba, Japan

Rayleigh-Bénard convection is one of the most famous non-equilibrium phenomena that occurs in fluid systems with a temperature difference between their upper and lower boundaries. The onset of convection is determined by the Rayleigh number, a dimensionless parameter that relates to buoyancy and thermal diffusion. If the Rayleigh number of the system is less than a critical value, convection does not occur. In contrast, when the Rayleigh number is above it, convection emerges.

In two-layer systems with an undeformed horizontal interface, Rayleigh-Bénard convection occurs with two types of patterns. One is mechanical coupling (MC), and the other is thermal coupling (TC). The vertical flow directions in the two layers are opposite in mechanical coupling, whereas they are the same in thermal coupling [1]. Various parameters, including the properties of fluids, the depth of layers, and the initial state, affect the final state.

We focus on the selection mechanism of thermal convection patterns in a symmetric two-layer system with an undeformed horizontal interface by varying the initial conditions in a two-dimensional hydrodynamic simulation. In this system, MC and TC patterns can be bistable in a certain parameter region [2,3]. Simulations were conducted with initial conditions corresponding to each coupling pattern (Figure 1). Based on the simulation results, we investigated the selection mechanism of the coupling patterns.

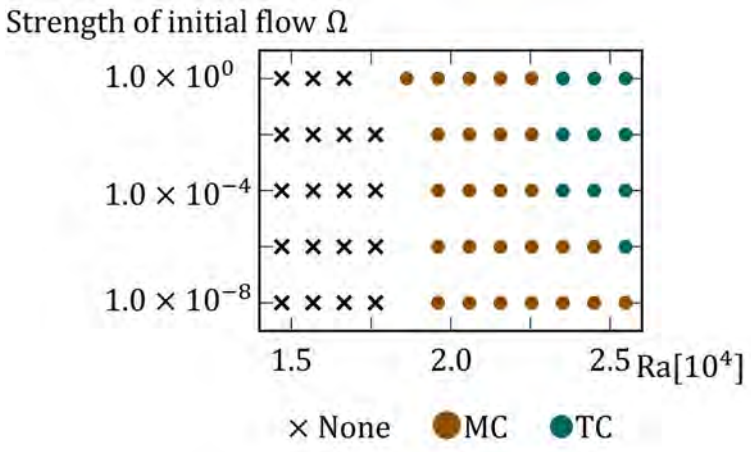

Fig. 1 : The Coupling pattern obtained from various initial conditions varied by Rayleigh number and the strength of the initial flow Ω.

References
1. C. Andereck, P. W. Colovas, M. M. Degen, and Y. Y. Renardy, *Int. J. Eng. Sci.*, **36**, 1451 (1998).
2. S. Rasenat, F. Busse, and I. Rehberg, *J. Fluid Mech.*, **199**, 519 (1989).
3. P. Colinet and J. C. Legros, *Phys. Fluids.*, **6**, 2631 (1994).

Onsager–Machlup variational principle for active systems

Kento Yasuda[1]

[1]College of Science and Technology, Nihon University

Onsager's variational principle (OVP) [1] and its extension, the Onsager–Machlup variational principle (OMVP) [2], provide a systematic way to derive dynamical equations for various soft-matter systems via the minimization of energy dissipation. In the current situation, where active matter attracts much interest in nonequilibrium physics, the application and extension of OMVP to such internally driven systems are required. In this presentation, we share our understanding of the OMVP framework and its perspective on active systems, including our contributions.

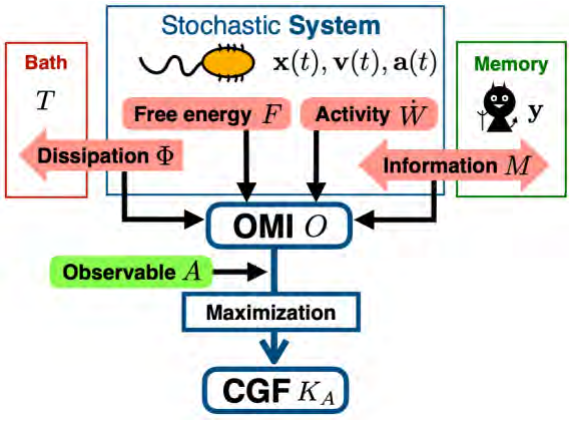

Figure 1 Schematic abstract of OMVP

Onsager claimed that the instantaneous velocity v at a state x can be determined by minimizing a quantity called the Rayleighian $R(x,v)$ with respect to the velocity v, which is referred to as OVP. The Rayleighian is constructed from the dissipation function Φ and the entropy production rate $\dot{\sigma}$, i.e., $R = \Phi - \dot{\sigma}$.

To make OVP a time-global principle, Onsager extended his principle with Machlup by introducing a functional called the Onsager–Machlup integral (OMI) [2]. The OMI $O[x(t), v(t)]$ is given by the time integral of the Rayleighian as $O = \int dt\, [R - R_{\min}]/(2k_B)$, where k_B is the Boltzmann constant and $R_{\min}$ is a minimum value of the Rayleighian with respect to velocity. The naive minimization of the OMI yields dynamics consistent with those obtained by OVP. In addition, the OMI essentially captures the system's thermal fluctuations, which can be extracted by observing the response to appropriate stimulation [3].

By including the active power P_a in the Rayleighian, the OVP and OMVP work even for active systems [4]. Examples include active Brownian particles [5,6], active stresses [4], and non-reciprocal activity [7]. Furthermore, we develop a framework for incorporating information processing in active particles via conditional probabilities [8].

The advantages of OMVP over typical Langevin stochastic differential equations are: (i) covariant at the level of the variational formulation, (ii) ease of introducing constraints via Lagrange multipliers, and (iii) avoidance of technical difficulties related to noise terms, the Itô–Stratonovich interpretation [9].

The points that are still unclear to us regarding OMVP are: (i) behavior beyond linear response, (ii) the validity of the saddle-point approximation [10] and how it works in bistable systems, (iii) how it can be utilized to find a systematic way of coarse-graining, and (iv) the formulation of a Noether theorem.

References

1. L. Onsager, Phys. Rev. 37, 405 (1931), M. Doi, Soft Matter Physics (Oxford University Press, 2013).
2. L. Onsager and S. Machlup, Phys. Rev. 91, 1505 (1953).
3. K. Yasuda, K. Ishimoto, and S. Komura, Phys. Rev. E 110, 044104 (2024).
4. H. Wang, T. Qian, and X. Xu, Soft Matter 17, 3634 (2021).
5. K. Yasuda and K. Ishimoto, Phys. Rev. E 106, 064120 (2022).
6. B. Zheng *et al.*, arXiv:2511.16178 (2025).
7. K. Yasuda, Phys. Rev. E 109, 064116 (2024).
8. K. Yasuda, K. Ishimoto, and S. Komura, arXiv:2510.13145 (2025).
9. A. W. C. Lau and T. C. Lubensky, Phys. Rev. E 76, 011123 (2007), T. Kuroiwa and K. Miyazaki, J. Phys. A: Math. Theor. 47, 012001 (2014), L. F Cugliandolo and V. Lecomte, J. Phys. A: Math. Theor. 50, 345001 (2017).
10. H. Touchette, Physics Reports 478, 1-69 (2009).

Dual Hamiltonian/Lagrangian Learning

Taito Nakajima[1] and **John J. Molina**[1]

[1]Dept. of Chemical Engineering, Kyoto University, Kyoto 615-8510, Japan

Physics-Informed Machine-Learning has transformed the way we analyze complex dynamical systems, allowing us to use partial/noisy data to infer the underlying laws/symmetries that determine the behavior of a system. This approach was pioneered in landmark papers introducing the Hamiltonian Neural Networks (HNN) [1] and the Lagrangian Neural Networks (LNN) [2], two physics-informed neural networks (PINN) that allow one to learn the hidden Hamiltonian/Lagrangian functions from phase-space/real-space trajectories. While Hamiltonian learning (e.g., HNN) allows one to leverage the symplectic structure of the phase-space, it usually requires knowledge of the canonical coordinates. Lagrangian learning (e.g., LNN) can be used when the canonical coordinates are unknown, but at the cost of losing the symplectic structure. Here, we present a dual Hamiltonian/Lagrangian Neural-Network, which explicitly encodes the Legrendre transformation between the Hamiltonian and Lagrangian functions. Thus, we have the best of both worlds and can learn Hamiltonians without requiring knowledge of the canonical coordinates. Our proposed framework outperforms both HNN and LNN, allowing for more efficient training and more robust predictions. Fig. 1 shows results for a simple harmonic oscillator, comparing our proposed LHNN with a standard HNN, as well as a baseline NN that does not incorporate any physical biases.

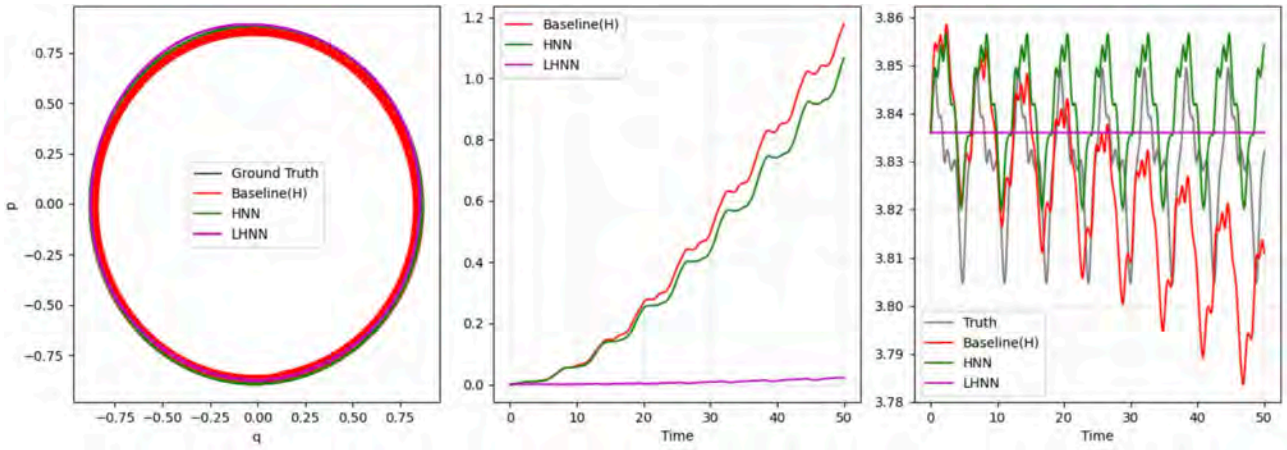

Fig. 1. Neural-Network predictions for a simple harmonic oscillator, comparing baseline NN, HNN, and LHNN. (left) Trajectory in phase space for a test orbit, (middle) Mean-squared error of the phase space trajectory, and (right) the conserved quantity, i.e., the learned energy function.

Acknowledgements

We acknowledge Takashi Taniguchi for fruitful discussions. This work was supported by a Grant-in-Aid for Scientific Research (JSPS Kakenhi No. 25H01536, 25K03185), as well as the JSPS Core-to-Core Program "Advanced core-to-core network for the physics of self-organizing active matter (JPJSCCA20230002)".

References

1. S. Greydanus, M. Dzamba, J. Yosinski: "Hamiltonian Neural Networks", *arXiv:1906.01563* (2019).
2. M. Cranmer, S. Greydanus, S. Hoyer, et al.: "Lagrangian Neural Networks", *arXiv:2003.04630* (2020).

Chemical Resonance, Beats, and Frequency Locking in Forced Chemical Oscillatory Systems

Hugh Shearer Lawson[1], Gábor Holló[2], Robert Horvath[3], Hiroyuki Kitahata[4], István Lagzi[1]

[1]Department of Physics, Institute of Physics, Budapest University of Technology and Economics, Budapest, Hungary
[2]Department of Fundamental Microbiology, University of Lausanne, Lausanne, Switzerland
[3]Nanobiosensorics Group, Institute of Technical Physics and Materials Science, Centre for Energy Research, Budapest, Hungary
[4]Graduate School of Science, Chiba University, Japan

In physics, the phenomena of resonance, synchronization, and beats are ubiquitous. The study and profound understanding of these physical systems have led to applications and technological advancements that have and continue to impact civilization. In our research, we aim to demonstrate that these properties also exist in a chemical environment (Fig. 1). The autonomous pH-oscillatory systems, namely sulfite–hydrogen peroxide and sulfite–formaldehyde–gluconolactone, were used to illustrate these concepts. In a continuous-flow stirred reactor, periodic forcing was achieved by superimposing a sinusoidal modulation on the reactant inflow. The correlation between the periodic beat time and the superimposed modulations is similar to the observed behavior of forced physical oscillations. Constructed mathematical models provided a qualitative analysis of the experimental results for the resonance and beat phenomena. The incorporation of periodic forcing into autonomous oscillatory systems produces a variety of oscillators with controlled frequencies, and the possibility of controlling chaotic chemical oscillation can therefore be realized.

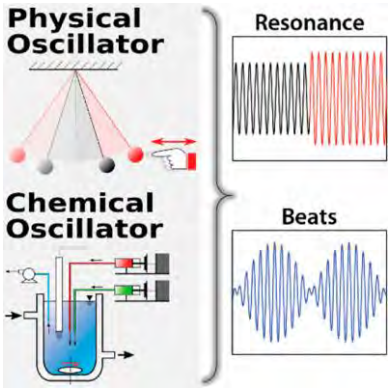

Fig. 1: Chemical resonance and beat phenomena in chemical systems.

Acknowledgements
This research was supported by the HUN-REN Hungarian Research Network, the National Research, Development and Innovation Office of Hungary (K146071), and JSPS Japan–Hungary Bilateral Joint Research Project (JPJSBP 120213801).

References
1. Hugh Shearer Lawson, Gábor Holló, Robert Horvath, Hiroyuki Kitahata and István Lagzi, Chemical Resonance, Beats, and Frequency Locking in Forced Chemical Oscillatory Systems. *Journal of Physical Chemistry Letters* **11**, 3014−3019 (2020).

Traveling defects as a precursor of the chimera states in a chain of non-locally coupled oscillators

Tianjing Zhou, Nariya Uchida

Department of Physics, Tohoku University, Sendai 980-8578, Japan

Chimera states in non-locally coupled oscillator networks [1] have garnered renewed attention due to its potential relevance to neuronal science. The phase delay in the coupling induces frustration, leading to the spatial coexistence of coherent and incoherent domains. While the onset and bifurcation scenarios of chimera states have been extensively studied, the large-scale spatiotemporal structure of multi-chimera states with a short coupling range remains to be fully understood. Here, we analyze the traveling defects observed between the synchronous and chimera states [2] using a non-local Sakaguchi-Kuramoto model in one spatial dimension:

$$\dot{\phi}_x = -\frac{1}{2R} \sum_{0<|s|\leq R} \sin(\phi_x - \phi_{x+s} + \alpha\pi)$$

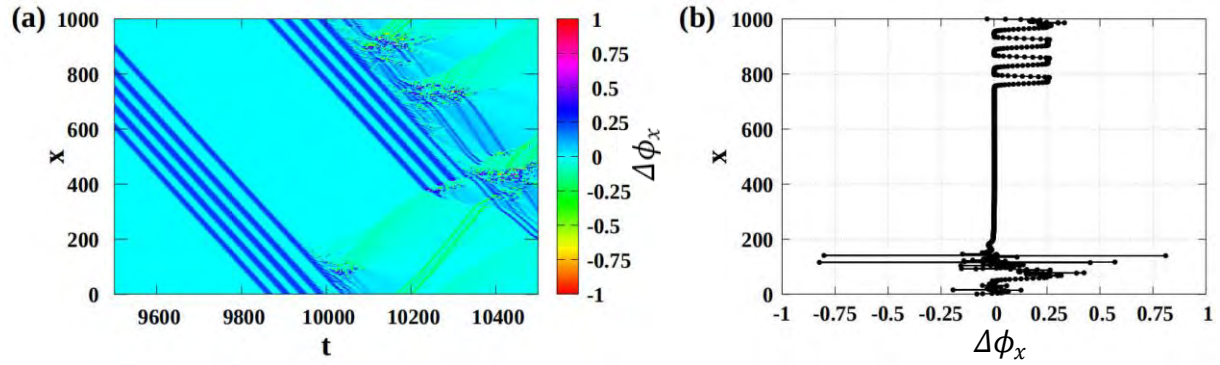

Fig.1: (a) Spatiotemporal map and (b) spatial profile of the phase gradient $\Delta\phi_x = \phi_{x+1} - \phi_x$ normalized to the range [-1,1]. The traveling wave patterns in (a) consist of solitary waves with a flat top as seen in (b). In (a), we see branching asynchronous clusters emerging from the instability of the traveling waves.

Figure 1 shows the spatiotemporal map and spatial profile of the phase gradient $\Delta\phi_x = \phi_{x+1} - \phi_x$ for the phase delay $\alpha = 0.439$ and coupling range $R = 5$. We identified a solitary wave with a flat top in the phase gradient profile [Fig. 1(b)]. The solitary waves travel at a constant speed [Fig.1(a)] and are identified with the traveling defects [2], which correspond to interfaces between q-twisted states. As seen in Fig.1(a), perturbations in the traveling defects develop into branching asynchronous clusters, serving as seeds for the chimera states. We performed a statistical analysis of the traveling defects by varying the phase delay α. As α increases, the fraction of samples exhibiting the traveling defects increases and peaks at $\alpha_c \approx 0.44$, where the system shows crossover to the chimera states. The number, width, and traveling speed of defects also increase with α up to α_c. We also studied the dependence of these characteristics on the coupling range and system size. These results shed new light on the emergence of chimera states in frustrated coupled oscillators.

References

[1] Y. Kuramoto and D. Battogtokh, *Nonlinear Phenom. Complex Syst.* **5**, 380 (2002).
[2] Y. Duguet and Y. L. Maistrenko, *Chaos* **29**, 121103 (2019).

Direct numerical simulations of Quincke Rollers in a bulk 3D system

Yusei Kitagaki, John J. Molina, and Ryoichi Yamamoto

Dept. of Chem. Eng., Kyoto Univ.

1 Introduction

Controlling the rheological properties of suspensions is crucial for industrial processes involving food and pharmaceutical products. Electrorheological (ER) fluids offer a promising solution by allowing viscosity control via external electric fields. Among these, suspensions of "Quincke rollers," in which dielectric particles undergo spontaneous rotation above a critical electric field, function as active ER fluids and have been studied for their potential for rheological modulation. Although recent 3D simulations indicate that the formation of particle chains due to dielectrophoretic forces—and the subsequent reversal of particle rotation within these chains—suppresses collective motion [1], the precise mechanism and its rheological consequences remain poorly understood. In this work, we used Direct Numerical Simulation (DNS) to investigate the dynamics of Quincke rollers, elucidating their three-dimensional microstructure and assessing the feasibility of controlling their rheological response.

2 Simulation Method

In this study, we adopted the Smoothed Profile Method (SPM)[2] to simulate suspensions of Quincke rollers. The SPM employs a profile function to smoothly represent the particle-fluid interface, thereby circumventing complex boundary treatments and significantly reducing computational costs. The fluid field was solved using the incompressible Navier-Stokes equations, while the translational and rotational dynamics of individual particles were computed using the Newton-Euler equations. To accurately capture the dynamics of Quincke rollers, the Newton-Euler equations incorporated electrostatic interactions alongside hydrodynamic and interparticle interactions.

3 Results and Discussion

In this study, we analyzed the dynamics of Quincke rollers in multi-particle systems under shear flow—a regime that has not previously been explored via simulation. As illustrated in Fig. 1, particles were dispersed within a simulation box subject to shear flow to determine the suspension viscosity. The resulting viscosity measurements, plotted against various electric field strengths and shear rates, are presented in Fig. 2. The data points representing conditions where Quincke rotation is active ($E/E_c > 1$)—specifically the red triangles, black circles, and pink diamonds—indicate a distinct reduction in viscosity. Conversely, in the regime where Quincke rotation is absent ($E/E_c = 0.6$), indicated by blue squares, an increase in viscosity driven by electrostatic interactions is observed at the lowest shear rate (leftmost data point). These findings are consistent with a previous experimental study [3], showing good qualitative agreement, particularly under conditions of low electric fields or high shear rates. However, discrepancies with the experimental results [3] were observed under high electric fields and low shear rates, an issue that requires further investigation in future work.

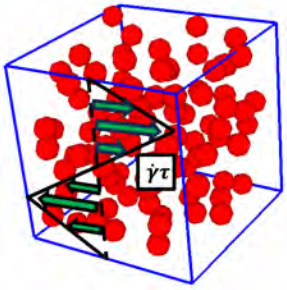

Fig. 1: Schematic of the simulation box.

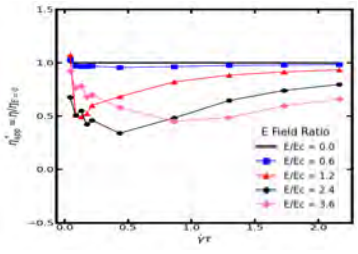

Fig. 2: Simulation results of the suspension viscosity under shear flow.

References

[1] D. Das and D. Saintillan: "On the absence of collective motion in a bulk suspension of spontaneously", *Soft Matter*, **19**, 6825 (2023).
[2] Y. Nakayama et al.: "Simulating (electro)hydrodynamic effects in colloidal dispersions:smoothed profile method", *Eur. Phys. J. E*, **26**, 361–368 (2008).
[3] E. Lemaire et al.: "Viscosity of an electro-rheological suspension with internal rotations", *J. Rheol.*, **52**, 769–783 (2008).

The Effects of Ordinary Viscosity in Chiral Shallow Water Model

Shota HOSONO, Kuniyasu SAITOH
Department of Physics, Kyoto Sangyo Univ.

Recently, active matter (e.g., living matters, Janus particles) has been investigated as one of the principal non-equilibrium systems. The coarse-grained active fluid model called the Toner-Tu-Swift-Hohenberg (TTSH) model describes the collective dynamics of self-propelled particles[1]. On the other hand, wave topology in the linearized chiral shallow water (CSW) model with odd viscosity is also essential concept to analyze the dynamics of topologically protected edge flows. According to previous studies, the edge flows such as the Kelvin wave and the Yanai wave observed at the equator of the Earth can be predicted by the difference of the Chern numbers between northern and southern hemispheres[2,3]. The eigenvalues of the effective Hamiltonian in the CSW model without ordinary viscosity, meaning that the system does not dissipate the energy and the effective Hamiltonian is Hermitian, are divided into two branches like a two-level system $E_{\pm} = \pm \mid \vec{s} \mid$ and a zero eigenvalue $E_0 = 0$, where a 3D real vector $\vec{s}$ is introduced as the Bloch vector[4]. This means that we can calculate the Chern numbers of each eigenmode easily by counting the winding numbers of the Bloch vectors. In contrast, if we introduce ordinary viscosity in the CSW model, the energy dissipation makes the effective Hamiltonian non-Hermitian, where the Bloch vectors are 5D complex vector.

The linearized TTSH+CSW model includes not only the ordinary viscosity term but also a 4-th order gradient term of coarse-grained velocity field. In addition, this model has an advection term which is associated with both the activity of active matter and the oscillation of edge flows[1,5] as the non-Hermitian terms. In this study, focusing on only the ordinary viscosity term, we consider the perturbation theory of the CSW model. Furthermore, we evaluate the complex eigenvalues, the non-Hermitian Chern numbers, the fidelity susceptibilities, and so on. The peaks of the fidelity susceptibilities correspond to either the critical points of the quantum phase transitions (like a topological phase transition) or the non-Hermitian exceptional points (EPs)[6,7]. We discuss how the perturbation of non-Hermiticity induced by the ordinary viscosity contributes to the CSW model.

[1] K. Kashyap *et al*., *arXiv*:2507.04890 (2025)
[2] Z. Zhu *et al*., *Phys. Rev. Res*. **5**, 033191 (2023)
[3] C. Tauber *et al*., *J. Fluid Mech*., vol. 868, p. R2 (2019)
[4] A. Souslov *et al*., *Phys. Rev. Lett*. **122**, 128001 (2019)
[5] H. Matsukiyo and J. Fukuda, *Phys. Rev. E* **109**, 054604 (2024)
[6] Y.-T. Tue, *et al*., *Quantum*, vol. 7, p. 960 (2023)
[7] G. Sun *et al*., *Front. Phys*., vol. 17(3), 33502 (2022)

Autonomous Noise-Rectified Locomotion via Self-Generated Viscosity Asymmetry

Bokusui Nakayama[1], **Yusuke Takagi**[2], **Ryoya Hirose**[1], **Masatoshi Ichikawa**[3], **Marie Tani**[1], **Ibuki Kawamata**[1], **Eiji Yamamoto**[2], **and Akira Kakugo**[1]

[1]Graduate School of Science, Kyoto University, Kitashirakawa, Sakyo, Kyoto, 606-8502, Japan
[2]Department of System Design Engineering, Keio University, 3-14-1 Hiyoshi, Kohoku, Yokohama, Kanagawa, 223 8522, Japan
[3]Graduate School of Integrated Sciences for Life, Hiroshima University, 1-3-2 Kagamiyama, Higashi-Hiroshima City, Hiroshima, 739-8511, Japan

Microscale transport often relies on thermal fluctuations, which are the most ubiquitous yet inherently random energy source. Converting such random fluctuations into useful work remains a central challenge in nonequilibrium physics and a key design goal for creating fluctuation-powered microdevices. In contrast to artificial systems, some biological systems employ self-regulated strategies that actively modify their rheological environments to create spatial asymmetries in mobility or diffusivity. Notably, certain bacteria can locally and nonuniformly modulate their surrounding medium, thereby achieving directed motion by rectifying thermal fluctuations, even in the absence of self-propelling structures such as flagella[1, 2]. In such systems, locomotion is governed by the internal orientation or configuration of the individual itself, enabling autonomous behavior and adaptive responses to complex environments.

Realizing this class of autonomous noise-filtering locomotion in controllable systems is essential for understanding how fluctuations can be harnessed as a functional energy source and for establishing design principles of fluctuation-powered active matter. Here we introduce self-viscophoresis as a new class of autonomous locomotion mechanism inspired by biological strategies, operating through noise-rectification. Rather than directly generating propulsion, a particle consumes energy to create an asymmetric viscosity field in its surroundings, as illustrated in Fig. 1. This field selectively filters the particle's thermal fluctuations, inducing a statistical bias in its stochastic dynamics, thereby producing persistent locomotion.

In this study, we experimentally demonstrate self-viscophoresis, where asymmetric colloidal particles in a thermoresponsive polymer solution generate viscosity gradients and undergo persistent locomotion under uniform illumination. Systematic analysis revealed that the locomotion velocity is proportional to the diffusivity difference across the particle surface. To elucidate the mechanism underlying the observed motion, we developed a minimal Langevin model incorporating equilibrium thermal fluctuations coupled to a dynamically updating temperature–viscosity field. The model shows that this viscosity asymmetry filters otherwise isotropic thermal fluctuations into a net drift, reproducing the observed dynamics without external forces or intrinsic self-propulsion.

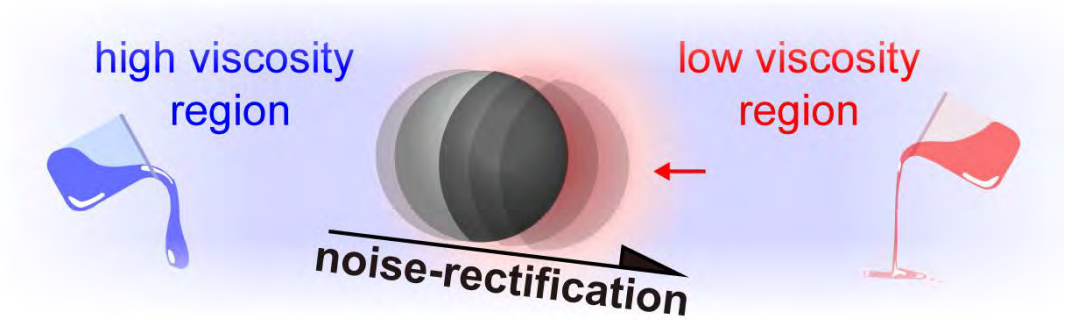

Fig. 1 Conceptual illustration of self-viscophoresis.

References

1. R. M. Brown, J. H. M. Willison, and C. L. Richardson, *Cellulose biosynthesis in Acetobacter xylinum: visualization of the site of synthesis and direct measurement of the in vivo process*, Proc. Natl. Acad. Sci. U. S. A. **73**, 4565 (1976).
2. S. C. Kuo and J. L. McGrath, *Steps and fluctuations of Listeria monocytogenes during actin-based motility*, Nature **407**, 1026 (2000).

Altruism in Epidemics

Mark P. Lynch[1], **S. K. Schnyder**[2], **J. J. Molina**[3], **R. Yamamoto**[3], **Matthew S. Turner**[4, 5]

[1] Mathematics of Systems CDT, University of Warwick, Coventry, CV4 7AL, UK
[2] Institute of Industrial Science, The University of Tokyo, Tokyo 153-8505, Japan
[3] Department of Chemical Engineering, Kyoto University, Kyoto 615-8510, Japan
[4] Department of Physics, University of Warwick, Coventry CV4 7AL, UK
[5] Institute for Global Pandemic Planning, University of Warwick, Coventry CV4 7AL, UK

Behavioural change such as social distancing or quarantining of infected individuals can affect the spread of infectious diseases. In models, individuals are typically treated either as passive agents which need to be forced to change their behaviour in response to the disease or their spontaneous behavioural response is assumed to be motivated by self-interest. In such frameworks, people show little concern for others and a significant reduction in social activity such as quarantining requires government enforcement. However, people are likely to be at least weakly altruistic and thus interested in protecting others. Unfortunately, little is known theoretically about how such altruism affects the course of epidemics.

Here we show using game theory that even extremely weakly altruistic individuals, valuing their own lives equivalent to roughly 100,000 others, can be expected to isolate when infected with a dangerous disease in a self-organised way, substantially suppressing epidemic spread, see Fig 1. Individuals self-isolate in order to avoid setting off chains of infections that they would perceive as costly to them even at such small altruism. Our results are robust to a moderate fraction of asymptomatic cases or completely selfish individuals. The resulting behaviour, while emerging from a complex optimisation problem, is simple enough that it could have evolved as a behavioural response in social animals, as well as being easy to communicate and understand for humans.

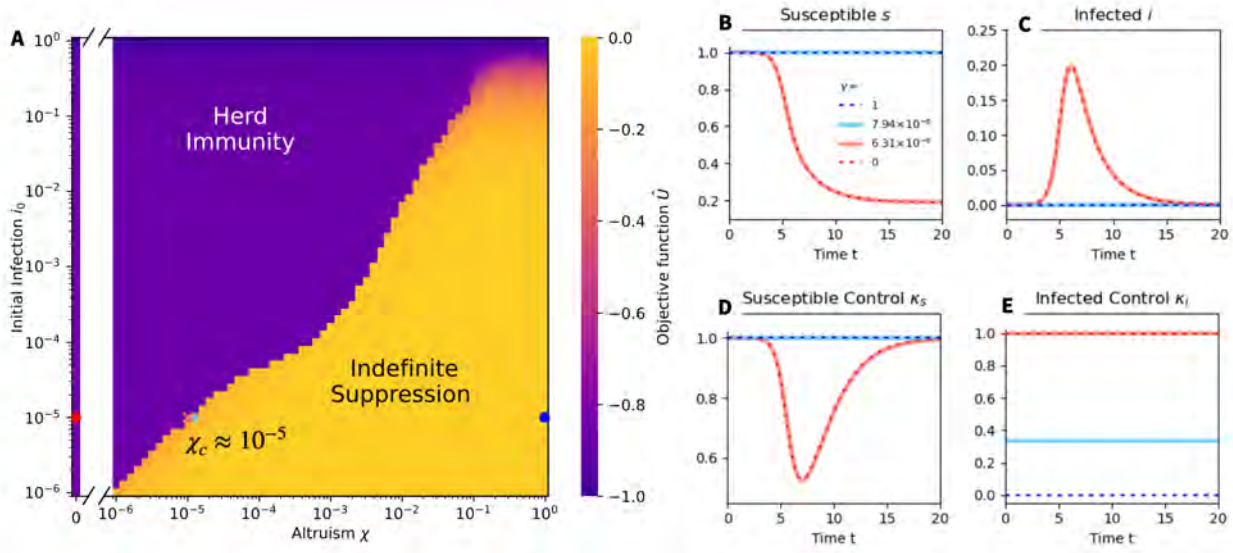

Fig. 1 : **The disease dynamics is is characterised by two Nash equilibria with vastly different outcomes:** A) Objective function $\hat{U}$ measuring expected infection and social distancing costs as function of altruism χ ($1/\chi$ corresponds to the number of people an individual considers as having the same aggregate value as their own life) and initial infected fraction of the population i_0. Certain infection without any social distancing corresponds to $\hat{U} = -1$. Symbols represent the parameter values for which the epidemic dynamics are shown in B, C), with corresponding social activities of susceptible and infected individuals shown in D, E). Indefinite Suppression is characterised by strong social distancing (i.e. low social activity) of infected individuals, thus containing the epidemic, and negligible social distancing of susceptible individuals. Herd Immunity is characterised by social distancing of susceptibles only, which is unable to contain the epidemic. The other disease parameters are $R_0 = 3$, and vaccination time t_f=100.

Exploring How We Explore: Statistical Patterns of Indoor Walking in Interactive Spaces

Sakurako Tanida[1], Claudio Feliciani[1], Akira Takahashi[2], Xiaolu Jia[3], Fernando Peruani[4], Hyerin Kim[5], Kensuke Yasufuku[2], Tetsuya Aikoh[5], and Katsuhiro Nishinari[1,2]

[1] The University of Tokyo, Japan
[2] Osaka University, Japan
[3] Beijing University of Technology, China
[4] CY Cergy Paris Université, France
[5] Hokkaido University, Sapporo, Japan

Human mobility has been widely studied using GPS and mobile phone data [1,2], revealing superdiffusive dynamics that characterize large-scale outdoor movements. In contrast, human motion in "exploratory" indoor environments, such as exhibitions or aquariums, can differ because people often move without fixed goals. Understanding the statistical properties of such wandering motion is essential for realistic modeling and for clarifying how people explore and interact within complex environments.

We analyzed indoor walking behavior recorded by a Bluetooth beacon system at Tokyo Big Sight, one of the largest exhibition facilities in Japan. Observations were conducted during the same three-day technology business event over two consecutive years. Beacon tags were distributed to a subset of participants, and receivers installed across the venue detected beacon IDs and timestamps, allowing reconstruction of discrete trajectories. For each trajectory, we computed three quantities: mean squared displacement (MSD), stay-duration distribution, and step-length distribution.

The MSD shows subdiffusive or slower growth, unlike the superdiffusive scaling reported in large-scale mobility. From seconds to tens of minutes, MSD increases as a power law with an exponent less than one, while it saturates at longer times due to the finite venue size. Stay durations follow a power-law decay with exponents near 2.0, consistent with previous observations of face-to-face contact durations [3]. In contrast, step lengths show an exponential distribution with characteristic lengths of several tens of meters. A simple lattice-based model demonstrates that the power-law nature of staying behavior can account for the observed MSD scaling, revealing a distinct regime of exploratory indoor human mobility.

Acknowledgements
We acknowledge the people for the discussion.

References

1. Gonzalez, M. C., Hidalgo, C. A., and Barabási, A.-L.: "Understanding individual human mobility patterns", *Nature* **453**, 779–782 (2008).
2. Rhee, I., Shin, M., Hong, S., Lee, K., Kim, S. J., and Chong, S.: "On the Lévy-walk nature of human mobility", *IEEE/ACM Transactions on Networking* **19**, 630–643 (2011).
3. Starnini, M., Baronchelli, A., and Pastor-Satorras, R.: "Modeling human dynamics of face-to-face interaction networks", *Physical Review Letters* **110**, 168701 (2013).

Stochastic Response of a Self-propelled Particle in the Chemical Concentration Gradients

Nobuhiko J. Suematsu[1,2]

[1]School of Interdisciplinary Mathematical Sciences, Meiji University
[2]Meiji Institute for Advanced Study of Mathematical Sciences (MIMS), Meiji University

Self-propelled particles in physicochemical systems exhibit diverse and functional behaviors, including taxis—directional movement in response to spatial gradients of environmental cues such as chemical concentration, light, or electric fields. Typically, these particles respond to local gradients by changing their direction. In contrast, many bacteria achieve chemotaxis without directly steering themselves. Instead, they alternate between straight runs and random tumbles, adjusting the frequency of each based on environmental conditions, which enables them to accumulate in favorable regions stochastically. In this study, we aimed to reproduce bacterial-like chemotaxis using physicochemical self-propelled particles experimentally and to uncover universal mechanisms underlying chemotactic behavior in both living and non-living systems.

We used phenanthroline disks, a type of self-propelled particle that swells on water due to reduced surface tension, which also alternates between movement and rest on an aqueous solution of iron ion, mimicking bacterial run-and-tumble (Fig. 1a). When placed on an iron ion concentration gradient, the disks accumulated more in low-concentration regions, demonstrating negative chemotaxis (Fig. 1b). Notably, each run was isotropic (Fig. 1c), indicating that the disks responded to chemical gradients without directional steering.

To explain this chemotactic mechanism, we suggested an agent-based random walker model in which the movement direction is randomly assigned, independent of environmental cues, but the run length depends on both position and direction:

$$x\,(n+1) = x\,(n) + l(x(n))\,(1 + b\cos\theta)\cos\theta$$

Here, $l(x)$ is a linear function of position ($l(x) = ax + l_0$), where a and b are constants representing "position bias" and "directional bias." Numerical simulations showed that the model can reproduce both positive and negative chemotaxis depending on the parameter ratio. Stochastic differential equation analysis explained this behavior and provided an expression for the steady-state distribution of particles.

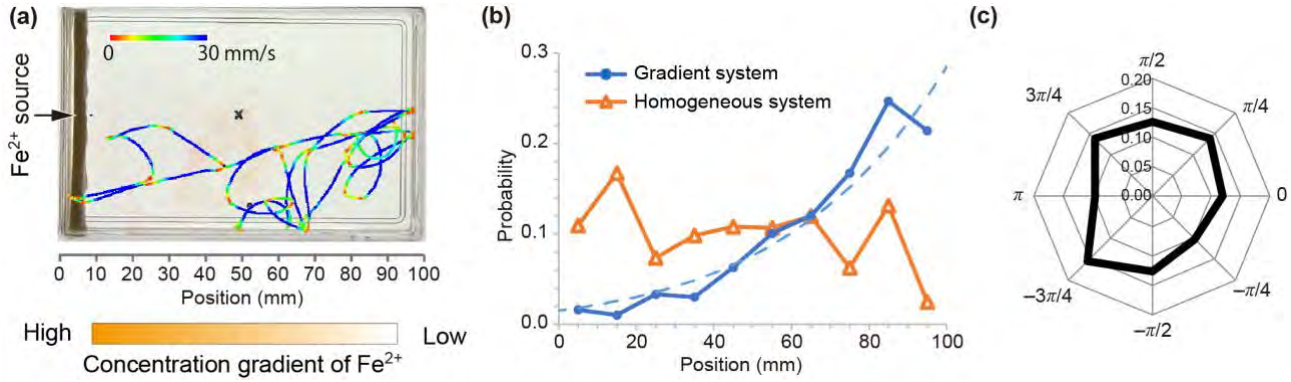

Fig. 1 Stochastic response of a self-propelled phenanthroline disk in the concentration gradient of Fe^{2+} [1]. **(a)** Trajectory of the movement of the particle, whose color indicates the speed of motion. **(b)** Probability distribution of the particles in gradient and homogeneous systems for chemical concentration. **(c)** Probability distribution of the direction of jump of a particle.

Acknowledgements
We appreciate Prof. Kota Ikeda, Prof. Kenta Odagiri, and Ms. Yuko Hamano for their contributions to making mathematical models, discussing the mechanism, and conducting experiments.

References

1. Hamano, Yuko; Ikeda, Kota; Odagiri, Kenta; Suematsu, Nobuhiko J.: "Reproduction of bacterial chemotaxis by a non-living self-propelled object", *Sci. Rep.* **13**, 8173 (2023).